

# We are IntechOpen, the world's leading publisher of Open Access books Built by scientists, for scientists

4,800

Open access books available

122,000

International authors and editors

135M

Downloads

Our authors are among the

154

Countries delivered to

TOP 1%

most cited scientists

12.2%

Contributors from top 500 universities



WEB OF SCIENCE™

Selection of our books indexed in the Book Citation Index  
in Web of Science™ Core Collection (BKCI)

Interested in publishing with us?  
Contact [book.department@intechopen.com](mailto:book.department@intechopen.com)

Numbers displayed above are based on latest data collected.  
For more information visit [www.intechopen.com](http://www.intechopen.com)



---

# Surface Modification of III-V Compounds Substrates for Processing Technology

---

Rodica V. Ghita, Constantin Logofatu,  
Constantin-Catalin Negrila, Lucian Trupina and  
Costel Cotirlan-Simioniuc

Additional information is available at the end of the chapter

<http://dx.doi.org/10.5772/67916>

---

## Abstract

Semiconductor materials became a part of nowadays life due to useful applications caused by characteristic properties as variable conductivity and sensitivity to light or heat. Electrical properties of a semiconductor can be modified by doping or by the application of electric fields or light; and from this view, devices made from semiconductors can be used for amplification or energy conversion. The compound semiconductor materials from III-V class experienced a qualitative leap from promising potential to nowadays technologic environment. The III-V semiconductor compounds are the material bases for electronic and optoelectronic devices such as high-electron-mobility transistors (HEMT), bipolar heterostructure transistors, IR light-emitting diodes, heterostructure lasers, Gunn diodes, Schottky devices, photodetectors, and heterostructure solar cells for terrestrial and spatial operating conditions. Among III-V semiconductor compounds, gallium arsenide (GaAs) and gallium antimonide (GaSb) are of special interest as a substrate material due to the lattice parameter match to solid solutions (ternary and quaternary) whose band gaps cover a wide spectral range from 0.8 to 4.3  $\mu\text{m}$  in the case of GaSb. The solid/solid interfaces could play a key part in the development of microelectronic device technology. In most of the cases, the initial surface of III-V compounds exposed to laboratory conditions is covered usually with native oxide layers. Various techniques for performing the surface cleaning process are used, e.g., controlled chemical etching, *in situ* ion sputtering, coupled with controlled annealing in vacuum and often these classic techniques are combined in order to prepare an eligible semiconductor surface to be exposed to a technological device chain. The evolution of surface native oxides in different cleaning procedures and the characteristics of as-prepared semiconductor surface were investigated by modern surface investigation techniques, i.e., X-ray photoelectron spectroscopy (XPS), atomic force microscopy (AFM), Rutherford backscattering spectrometry (RBS) combined with electrical characterization. Surface preparation of semiconductors in particular for III-V compounds is a necessary requirement in device technology due to the existence of surface impurities and the presence of native oxides. The impurities can

affect the adherence of ohmic and Schottky contacts and due to thermal decomposition of native oxides (e.g., GaSb) it also affect the interface metal/semiconductor. The practical experience reveals that the simple preparation of a surface is a nonrealistic expectation, i.e., surface preparation is a result of combined treatments, namely chemical etching and thermal treatment, ion beam sputtering and thermal reconstruction procedure.

**Keywords:** III-V compounds, surface oxides, surface etching, XPS, AFM, RBS, metallic nanolayers

---

## 1. Introduction

Semiconductor materials became a part of nowadays life due to useful applications caused by characteristic properties as variable conductivity and sensitivity to light or heat. Electrical properties of a semiconductor can be modified by doping or by the application of electric fields or light; and from this view, devices made from semiconductors can be used for amplification, switching, and energy conversion. A pure semiconductor is not very useful as it is neither a very good insulator nor a very good conductor. The conductivity of semiconductors may easily be modified by introducing impurities into their crystal lattice, implying a controlled doping process. The materials suitable as dopants depend on the semiconductor nature (e.g., for silicon the common are group III *p*-type dopants, acceptor impurities and group V-*n*-type dopants, donor impurities). Electrical conductivity is a consequence of the presence of electrons in states that are partly delocalized, however in order to transport electrons a state must be partially filled. The energies of these quantum states are critical due to the fact that a state is partially filled only if its energy is near the Fermi level (Fermi-Dirac statistics). In a semiconductor, the number of partially filled states is increased by doping or by gating move either the conduction or valence band closer to the Fermi level. Electron-hole pair generation can appear when a semiconductor is exposed to ionizing radiation, and as a consequence an electron is excited out of its energy level and consequently leaving a hole. The number of electron-hole pairs in a steady state at a given temperature is established by quantum statistics, where the precise quantum mechanism of generation and recombination are governed by conservation laws of energy and momentum. In electronics, the applications are based in the most part on current flow through material in different *p-n* junction geometries. Heterojunctions occur when two different doped semiconducting materials are jointed in an intimate contact. Operating different heterojunction devices is based on the current flow between *p*-type and *n*-type regions caused by an applied electric field. In general, a difference in electric potential would cause the appearance of a nonequilibrium situation that can introduce electrons and holes to the system, which interact through ambipolar diffusion. The change of thermal equilibrium as a result of a temperature difference or to exciting photons caused the process of generation and recombination of carriers (i.e., change of electrons and holes number). In certain semiconductors, exciting electrons relax by emitting light and this process is the fundament of light-emitting diode operation. Certain semiconductors have large thermoelectric power factors, therefore they can be used in thermoelectric generators (e.g., thermoelectric coolers).

The compound semiconductor materials from III-V class experienced a qualitative leap from promising potential use in semiconductor devices as they were viewed at the mid of twentieth century to extensively fabrication in optoelectronics industry at the beginning of twenty-first century. As it was stated Ref. [1], III-V semiconductor compounds are the material bases for electronic and optoelectronic devices as high-electron-mobility transistors (HEMT), bipolar heterostructure transistors, IR light-emitting diodes, heterostructure lasers, Gunn diodes, Schottky devices, photodetectors, heterostructure solar cells for terrestrial and spatial operating conditions, microwaves devices, electro-optical modulators, and frequency-mixing components. In principal, the main characteristics of these devices are dependent on the physical properties of III-V materials and their solid solutions, mostly ternary and quaternary alloys. It is to be remarked the presence of quantum effects in quantum heterostructure devices design that extended the operating and reliability features. In order to exploit this flexibility of III-V materials it is necessary to use a band parameter data base as the starting point to analyze, compute, and simulate the operation of a device in its way to a reliable technology. The III-V compounds of interest are those between Al, Ga (group III) and P, As and Sb (group V), i.e., AlP, AlAs, AlSb, GaP, GaAs, GaSb, InP, InAs, InSb and their ternary and quaternary solid solutions, e.g.,  $\text{Al}_x\text{In}_{1-x}\text{P}$ ,  $\text{Al}_x\text{Ga}_{1-x}\text{As}$ ,  $\text{Al}_x\text{In}_{1-x}\text{As}$ ,  $\text{Al}_x\text{Ga}_{1-x}\text{Sb}$ ,  $\text{Al}_x\text{In}_{1-x}\text{Sb}$ , InGaAsP, AlGaPAs, GaInAsSb, AlGaAsSb. Isoperiodic epitaxial heterostructures composed of quaternary solid solutions as GaInAsP/InP, GaInAsSb/GaSb, or AlGaAsSb/GaSb are the basis for optoelectronic devices of a given spectral range extending over a wide spectrum and their study determined a progress in semiconducting band engineering. Some important characteristics of classic III-V compounds are the lattice structure of zincblende type, the same space group  $T_d^2-F-43m$ , lattice parameter  $a_0$  at 300 K in the range (5.451 Å, for GaP to 6.47 Å, for InSb) and energy gap at 300 K in the range (0.17 eV, for InSb to 2.45 eV, for AlP with different direct and indirect features. Also, an important class of wurtzite structure is AlN and GaN based compounds that have been used for short wavelength light emitters. It is worth to mention that incorporation of N and In into GaAs lattice results in lowering the band gap energy of GaAs, whereas minimizing the strain as In tends to increase and N tends to reduce the lattice constant of GaAs. The lattice matching InGaAsN layers to GaAs conducted to first (In)GaAsN lasers presented in 1996 [2].

Among III-V semiconductor compounds, gallium arsenide (GaAs) and gallium antimonide (GaSb) are of a special interest as a substrate material due to the lattice parameter match to solid solutions (ternary and quaternary) whose band gaps cover a wide spectral range from 0.8 to 4.3  $\mu\text{m}$  in the case of GaSb [3]. Regarding devices perspectives, GaSb have shown applications in laser diodes with low threshold voltage [4], photodetectors with high quantum efficiency [5], high frequency devices [6] or to high efficiency thermophotovoltaic (TPV) cells [7]. In this perspective, GaSb is a III-V semiconductor compound with zincblende crystal structure and has an energy gap of 0.726 eV and is worth to mention that the structure GaAs/GaSb had set a record for solar cell efficiency of 35% opening a new era for photovoltaics applications. We can say that the GaSb photosensitive structures offers the possibility of an almost total conversion of sun energy from visible spectrum to heat transform in electricity by TPV effect. Another property to mention is related to GaSb lattice limited electron mobility that is greater than GaAs, which make it available in fabrication microwave devices. The property of GaSb band structure related to the spin-orbit splitting of the valence band, that is almost equal

to the gap conducted to high hole ionization coefficients leading to an improvement of signal-to-noise ratio at  $\lambda > 1.3 \mu\text{m}$  in AlGaSb/GaSb avalanche photodetectors [5]. GaSb-based devices are candidates in infrared (IR) imaging sensors, fire detection, and monitoring environmental pollution. We remark that the absorption wavelength of different industrial toxic gases are in the IR range where GaSb devices are recommended due to band gap structure, the near IR regime is also suitable for biological and medical applications. Some interesting aspects of GaSb are related to the fact that undoped semiconductor is always of *p*-type irrespective of growth procedure, and sulfur-doped GaSb is the only III-V compound with high concentration of donor-related deep traps (*DX* centers) at atmospheric pressure [3]. At this status, the GaSb compound study is of interest due to effort for understanding material preparation and processing in order to develop a competitive technology for optoelectronic devices, in our case the competitive Schottky devices for terrestrial applications. As it was stated, the solid/solid interfaces could play a key part in the development of microelectronic device technology. In most cases, the initial surface of III-V compounds exposed to laboratory conditions is covered usually with native oxide layers. In this view, the III-V surface oxides are unstable from a chemical point of view. Various techniques for performing the surface cleaning process are used, e.g., controlled chemical etching, *in situ* ion sputtering, cycle of controlled annealing in vacuum and often these classic techniques are combined in order to prepare an eligible semiconductor surface to be exposed to a technological device chain.

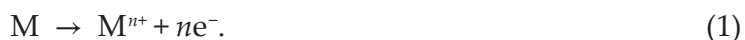
Generally speaking obtaining good ohmic contacts on semiconductor material surfaces is dependent on the ability of the cleaning procedure to remove the native oxides and in the case of III-V compound semiconductors to keep the surface stoichiometry. Deposition of metallic layers on clean semiconductor surface in order to obtain good ohmic or Schottky contacts is an important goal for device and structure preparation [8]. The evolution of surface native oxides in different cleaning procedures and the characteristics of as-prepared semiconductor surface were investigated by modern surface investigation techniques, i.e., X-ray photoelectron spectroscopy (XPS), atomic force microscopy (AFM), Rutherford backscattering spectrometry (RBS) combined with electrical characterization.

## 2. Preparation and investigation techniques

The III-V semiconductor compounds as solid state materials are covered by a surface that acts as an interface to the surrounding environment. Generally speaking, the surface modification is the action upon the surface of a material by bringing physical or chemical characteristics that are slightly different from the ones initially found on the surface. Another view of surface modification is represented by surface functionalization that introduces chemical functional groups to a surface. In this way, materials with functional groups on their surface can be designed from substrates with standard bulk material properties, e.g., in semiconductor industry. Commonly speaking, the surface modification is made to the semiconductor materials for altering characteristics as roughness, surface energy, or reactivity. From this point of view, surface engineering involves the alteration for the surface phase properties in order to reduce degradation over time. Surface engineering techniques that are commonly used in

electronics and optoelectronics implied in this work, the controlled action on semiconductor surface by chemical and physical etching.

Etching procedure is used in microelectronics to chemically remove layers from the surface of a wafer during fabrication. Etching is a peculiar and important process where generally the wafer undergoes many etching steps before it is complete. From a historical point of view, chemical etching or so-called wet etching, plays an important role in both preparation and the utilization of thin films. In this perspective, for thin film deposition, e.g., metallic layers, the substrate has to be first suitable prepared, i.e., the removal of a work damaged surface layers or by creating a relief structure of specific geometry. In both cases, the method used is either a chemical polish etching or is a structural etching. One important application of chemical etching is in the structural characterization of materials, especially in detection of lattice defects in semiconductors, in the distribution study of localized impurities, in the determination of layer structures or *p-n* junctions, and last but not least in the composition determination. Regarding the chemical etching [9], the simplest way involves only the dissolution of the material in a solvent without changing the chemical nature of the dissolved species. Most part of etching processes involves one or more chemical reactions. A true etching reaction is characterized by the formation of an etchant product that must be soluble in the etchant medium. Different types or reaction involved are of oxidation-reduction type, electrochemical type, complexation, and gas phase etching. A redox etching process implies conversion of the material being etched to a soluble higher oxidation state:



It is worth to mention that complex formation is frequently involved in etching processes, often in conjunction with a redox act, where the formation of a complex ion or molecule is accompanied by solubilization in the etchant medium. Gas phase etching may involve vaporization of the material that has been etched in a vacuum or in inert atmosphere. In another situation, gas phase etching is involving the reaction of gaseous etchants with the surface to produce volatile products. Etching reactions are characterized by a process involving several sequential steps [10]. The dissolution kinetics is depending on the nature of the rate-limiting step of the process in the following view. If the rate of this step is a function of the chemical reactivity of the species involved, the process is said to be activation limited. On the other hand, if the rate is determined by the velocity at which a fresh reactant can be supplied to the surface, the process is said to be diffusion limited. It is observed that an increase in etching temperature is a cause for change in the etching kinetics [11]. Other factors that can influence the etching process are the presence of catalytic species in the etchant, solution agitation, or localized solution heating. It is important to mention that adsorption and desorption processes can affect the etching kinetics, i.e., adsorption of a reactant from the etchant solution onto the substrate may produce surface complexes that can facilitate the etching process. The kinematic aspect of etching is related to the tendency of various crystallographic planes to etch at different rates. Various orientations of single-crystal semiconductors may etch differently in a given etchant and substrates with nonuniform roughness exhibit large differences in etch rates. It is remarkable that the simplest etching technique is liquid chemical immersion or dip etching. In this process, mechanical agitation is usually desirable, because it improves

the uniformity and control of chemical etching by enhancing the spread of etching solution at the solid surface. Mechanical agitation generally avoids local overheating in case of exothermic reactions a fact that conduced to a control of etching rate. The addition of a surface-active agent to etch solution can prevent bubble accumulation (e.g., formation of  $H_2$  bubbles that can inhibit uniform etching).

The subject of contamination and cleaning of surfaces before and after etching is closely related with practical etch process. Surface contamination as related to etching has two aspects: (a) initially presence of contaminants and their removal prior to etching, and (b) residual contaminants arising from etching treatments and their removal as a post-etch step. Contamination prior to etching consists of particulate materials, organic residues, or inorganic surface films different from the semiconductor to be etched. Particulate removal is generally accomplished by ultrasonic treatment in cleaning solution, use of compressed gas jets, application of liquid sprays or jets, or by mechanical means as brushing. Organic residues are removable down to monolayer levels by dissolution in suitable organic solvents (e.g., trichloroethylene, acetone or propranolol) or by vapor refluxing in organic solvents as azeotropic solvent mixtures. Complete removal is generally possible only by plasma etching, glow discharge sputtering, or chemical reaction leading to dissolution. Inorganic surface films (an example may be oxides) had to be attacked by specific chemical reagents designed to produce soluble reaction products that can be flushed away. While the treatments of initial contaminants are generally simple, the effective removal of residual trace contaminants resulting from etching process is more difficult to accomplish. It is remarkable that the surface contaminants are very critical in technologies where high-temperature processing may cause residual surface impurities to penetrate into the substrate and to be the origin of undesirable effects as electrical instability of semiconductor devices. Surface cleaning by glow discharge sputtering techniques is effective on semiconductor surface. Most organic surface contaminants are removable by chemical sputtering in  $O_2$  and sputter etching in  $Ar^+$  removes residual oxide layers on metals. However, surface recontamination due to backscattering or ion migration can occur during RF sputtering treatments, unless carefully optimized processing conditions are employed. Ultrahigh vacuum heating after sputter cleaning is effective for desorbing gases that may become incorporated into substrates surface during operation [12]. Plasma etching is to be noted as one of the most effective methods for surface decontamination with application to semiconductor device processing. It is remarked that for surface cleaning two aspects are important, i.e., terminal treatment and storage of the cleaned material. The final rinse in wet cleaning and etching process is usually in water. In this view, cleaning procedure is used only in deionized and distilled water in order to avoid contamination. High-purity electronic-grade isopropyl alcohol is a good alternative final rinse after DIW (deionized water). Storage of cleaned materials should be minimized, but if the storage is necessary, should be used chemically cleaned closed glass containers (e.g., Petri dishes) kept in a contamination-free clean-room ambient. In etching processes, selectivity is an important factor in experimental applications. In III-V compound semiconductors etching reactions are complicated due to the effect of crystallographic orientations. Chemical etching of GaAs, GaP, or GaSb proceeds by oxidation-reduction complex reactions analogous in the main part with the mechanism for Si and Ge etching. The most common etchant in this system is based on  $H_2SO_4-H_2O_2-H_2O$  in

different volume ratios as a function of orientation-dependent etching characteristics. In this work will be analyzed also chemical etchants in citric acid base or sulfur base organic and inorganic etchants for GaAs or GaSb.

Physical action on the surface, the so-called “dry etching,” refers to the removal of material typically a masked pattern of semiconductor by exposing it to the bombardment of ions, e.g., plasma of reactive gases that dislodge portions of the material from the exposed surface. Dry etching is a process with characteristics of anisotropy and is particularly useful for semiconductors which are chemically resistant.

In modern VLSI (very large scale integration) processes, plasma etchers, i.e., charged ions or neutral atoms and radicals, can operate in several modes by adjusting plasma parameters. Plasma etching operates at pressure in the range (0.1–5) torr by producing free radical, neutrally charged, that react at the substrate surface in a process with an isotropic character. In plasma, there are present different species as electrons, ions, radicals, and neutral particles that are constantly interacting with each other. In plasma etching interaction can be divided into two types, namely, generation of chemical species and interaction with the surrounding surfaces. The operation mode of plasma system will change if the operating pressure changes and it is also dependent on the reaction chamber geometry. The main factors that influence the plasma process are electron source, pressure, gas species, and vacuum. The success of a plasma etching process is dependent on appropriate etch chemistry that will form volatile products with the exposed semiconductor to be etched. The surface temperature also affects the reaction of products. The plasma etching process is also affected by different properties such as volatility, adsorption, or chemical affinity. In semiconductors the processing plasma etching can be used to create different patterns on a fabrication chain playing a major role in microelectronic production.

Ion milling or sputter etching uses lower pressures in the range of  $10^{-4}$  torr and it acts by the bombardment of the substrate with energetic ions of noble gases, more often  $\text{Ar}^+$ , which knock atoms from the substrate by momentum transferring. This process performed by ions which act approximately from one direction has a highly anisotropic character but it tends to present a poor selectivity characteristic.

Reactive-ion etching (RIE) operates under pressure conditions intermediate between sputter and plasma etching, i.e., in the pressure range  $10^{-3}$ – $10^{-1}$  torr. The upgrade technique is deep reactive-ion etching (DRIE) that modifies RIE technique to produce deep, narrow features. From this point of view, DRIE is a highly anisotropic etch process to create deep penetration, steep-sided holes and trenches in substrates with high aspect accuracy. This technique was developed initially for microelectromechanical systems (MEMS) which require these features. There are two main technologies for high-rate DRIE, namely, cryogenic and Bosch, and both of them can fabricate truly vertical walls, but in practice, the walls are slightly tapered, e.g.,  $88^\circ$  (“reentrant”) or  $92^\circ$  (“retrograde”).

It is worth to mention that the dry etching technology is expensive compared to wet etching procedure, but regarding the resolution in thin film structures is to be consider as possible solution.



Surface cleaning by physical means, in our case, sputtering technique, can also be effective in the case of removal of oxide layers on III-V semiconductors by Ar<sup>+</sup> ion beam sputtering. Sputtering is a process whereby particles are ejected from a target by bombardment of gas ions. The incident ions set off collision cascades in target and the number of atoms ejected from target (sputter yield) is depending on ion incident angle, ion energy, ion mass, target atom mass, and surface binding energy of target atoms. Ion sputtering has a defined threshold energy depending on binding energy of surface atom with a value in the range 10–100 eV. The process of atom removing from by sputtering using inert gas is an ion etching process. For semiconductors (peculiar for III-V compounds), ion sputtering is used to etch the target and sputter etching is chosen in cases with a high degree of etching anisotropy and where selectivity is not a concern. For Ar<sup>+</sup> ion beam, sputtering of carbon and oxygen presence from GaAs, GaSb, or GaP surface is needed an accelerating voltage of 0.5 kV for few minutes. The sputtering process is an *in situ* cleaning procedure where the usual Ar<sup>+</sup> accelerating voltage is in the range 1–3–5 kV and ion beam current *I* in the range 25–50–100 μA. The rate used for Ar<sup>+</sup> ion beam voltage is usually 1 kV and the sputtering time used for cleaning is in the range 1–5 minutes. The main advantages of sputtering are related to the fact that it is a rapid and *in situ* cleaning process (the process has a high rate cleaning degree). The important disadvantages are related to the fact that at the semiconductor surface may appear stoichiometric modifications and Ar<sup>+</sup> ion can damage the semiconductor by penetrating the lattice. For III-V compounds in Ar<sup>+</sup> ion sputtering process the Ga atoms are preferentially present on the surface (e.g., GaAs, GaSb, GaP), and it is necessary for a thermal reconstruction treatment at temperatures in the range 200–400°C for few hours. In other words, one major drawback of sputtering as an etching cleaning technique for semiconductors is the wafer damage.

In the case of III-V semiconductor compounds technology, have been used combined *ex situ* techniques as chemical etching and thermal treatments cycles and *in situ* cleaning as sputtering and reconstruction treatment in order to prepare a semiconductor surface for device technology requirements.

The characteristics of a native semiconductor surface and of a prepared surface for different technological device requirements may be investigated by surface characterizing techniques, i.e., XPS, AFM, SE, or RBS.

X-ray photoelectron spectroscopy (XPS) is a sensitive quantitative spectroscopic technique that detects all elements and can be used to analyze the surface chemistry of a material in its as-received state or of a surface exposed to different chemical or physical treatments. The presence of native oxides (e.g., GaAs, GaSb) with a structure and a well-defined composition may be analyzed by angle-resolved XPS (ARXPS), for example in a XPS SPECS system. It is worth to say that a typical XPS spectrum is a plot of the number of electron detected (*y*-axis) versus binding energy of detected electrons (*x*-axis). Each element is characterized by a set of XPS peaks at a specific binding energy values that directly identify each element that is situated inside or on the surface of the as-analyzed material. The characteristic spectral peaks correspond to the electron configuration of the electrons within the atoms, e.g., 1s, 2p, 2p, 3s, 3d, etc. The number of detected electrons in each characteristic peaks is related to the amount of element within the XPS sampling volume. In order to obtain atomic percentage values, each raw XPS signal must be corrected by dividing its signal intensity by a relative

sensitivity factor (RSF) and normalized over all the elements detected (except hydrogen that is not detected). In order to count the number of electrons during acquisition of spectrum with a minimum of error, the XPS detectors have to operate under ultra-high vacuum (UHV) conditions ( $p \sim 10^{-9}$  torr) because the electron counting detectors in XPS instruments are typically 1 m away from the material irradiated with X-rays and this is the condition why this long path length for detection requires such low pressures. In this work, the XPS recorded spectra were obtained in the as-mentioned SPECS Spectrometer based on a Phoibos analyser with monochromatic X-rays emitted by an anticathode of Al (1486.7 eV). The hemispherical analyzer operated in the constant energy mode with a pass energy of 5 eV, giving an energy resolution of 0.4 eV, which was established as FWHM (full width half maximum) of the Ag  $3d\ 5/2$  peak. The analysis chamber was maintained as specified at ultrahigh vacuum conditions ( $\sim 10^{-9}$  torr). The recorded spectra were processed using Spectral Data Processor v 2.3 (SDP) software, and the good fit for experimental data is ensured by a specific ratio between a Lorentzian and a Gaussian shape in the deconvolution of XPS peaks. The XPS measurements were carried out at different TOA (take-off angles), where TOA is defined as well as its description in the ASTM E 673-98 related to standard terminology regarding surface analysis. In this perspective TOA represents the angle between the beam of emitted photoelectrons and the sample surface. As regarding surface sensitivity, we remark that XPS detects only those electrons that have actually escape from the sample into vacuum of the instrument, and reach the detector. The photoelectron that escapes from the sample into the vacuum actually travels through the sample. These photo-emitted electrons may undergo inelastic collisions, recombination, excitation of the sample, recapture, or trapping in various excited states within material, where all these processes can reduce the number of escaping photoelectrons. These effects are present as an exponential attenuation function as the depth increases, the result is that the signals detected from analyzed element at the surface is much stronger than the signals detected from the same element deep under sample surface. The consequence is that the XPS signal has a characteristic of an exponentially surface-weighted signal and may be used to estimate different elements depths in layered materials. The main characteristic of XPS analysis as a surface-sensitive investigation technique was intensively used for the quantitative analysis of as-received semiconductor surface, namely the structure of native oxides developed at the surface of GaAs, GaSb, GaP single crystals. The effect of different surface preparation procedures was also put into evidence by XPS and ARXPS analyses.

Atomic force microscopy (AFM) is a powerful technique for investigating the surface morphology of materials at nanoscale level. AFM can image the sample surface topography with extremely high—up to atomic—resolution which is comparable with the scanning electronic microscopy (SEM). The advantage of AFM compared to SEM is that the measurement is made in three dimensions. The vertical resolution can be on the order of Angstroms while the lateral resolution depends on the tip radius. The working principle of AFM is based on force measurement between a small tip and a sample surface. The tip placed at the end of a silicon cantilever can have a nominal radius of curvature at the tip apex of 10–40 nm. High-resolution images can be obtained with cantilevers having an extremely sharp diamond-like carbon tip with typical curvature radius of 1 nm [13]. The image of the sample surface is obtained by monitoring the bending of the cantilever as it scans along topographic features. The cantilever displacement is

measured by detecting the deflection of a laser beam which is reflected from the back side of the cantilever and collected in a photodetector. The output of the photodetector is used to control the cantilever deflection by adjusting the height of the probe via a piezoelectric actuator.

Depending on tip-sample separation during scanning three different modes of operation exists: noncontact, intermittent contact, and contact. The noncontact mode operates at distances between 0.1 and 10 nm where attractive Van der Waals force occurs between tip and sample surface. In this mode the tip oscillates above the surface during scanning and a feedback loop is used to track changes in the amplitude due to tip-sample interaction. The advantage of this operating mode is the low force applied on the sample, which can be important when soft surfaces are investigated, but usually images with lower resolution are obtained. At distances of 0.5–2 nm between the tip and surface sample the AFM works in intermittent contact. In this mode the tip is oscillating at its resonance frequency and just barely touching the surface while is at the bottom of its oscillation. Thus, compared with noncontact and contact mode, higher resolution and greatly reduced lateral force are obtained, respectively. As the tip moves closer to sample surface, at distances smaller than 0.5 nm, the tip-sample interaction force becomes predominantly repulsive due to the repulsion generated by the overlap between the electron clouds of the tip and surface atoms. This is known as the contact mode, which is the best mode for scanning hard and flat surfaces. In this study the surface morphology and roughness of the samples were investigated by atomic force microscopy using an MFP 3D SA, Asylum Research microscope operated in the intermittent contact mode under ambient atmosphere. The tip used had a radius of curvature of 10 nm, spring constant  $k = 3.4$  N/m and resonance frequency about 107 kHz.

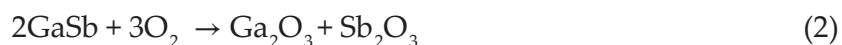
Rutherford backscattering spectrometry (RBS) is an analytical technique used in materials science. The elemental composition of thin metals layers were investigated by RBS using a  $^4\text{He}^{++}$  beam extracted from the Alphatross ion source of the 3 MV Tandetron accelerator of IFIN-HH. The beam energy was 3 MeV. The alpha particles were detected with a passivated ion implanted silicon detector. The detector had an energy resolution of 16 keV and was placed at  $165^\circ$  with respect to the beam direction. The solid angle was 1.641 mSr. In order to avoid channeling effects the sample was tilted at  $7^\circ$  with respect to the beam direction. The elemental concentrations and the layer thickness were determined using code RUMP [14] by fitting the RBS experimental spectrum of the sample. The RBS analysis was corroborated with XPS data in obtaining the depth profile of AuGeNi/n-GaSb, the metal layers being vacuum deposited on a clean n-GaSb surface prepared by chemical etching. The depth profile shows that Au, Ge, and Ni are uniformly distributed in matrix and an Au-Ga alloy that assures a good ohmic contact was detected.

### **3. Initial stage of the III-V semiconductor surface-presence of native oxides**

A major problem to be overcome in the technology of III-V compounds is the poor quality of oxide/semiconductor interfaces [15]. For devices of MIS (metal-insulator-semiconductor), the

presence of a stable interface containing a low density of electronic defect states around band gap is essential for device operating characteristics. The main source of defects is known to be the oxidation of III-V semiconductor surface and in particular at GaSb surface the oxidation is an exothermic reaction. Generally speaking the III-V surface oxides are chemically unstable in air. It is stated that for GaSb [16], although the native oxides can be stabilized against chemical attack, this stabilization procedure requires high temperatures over 600°C, a temperature above the allowed temperature range for some device structure technology. In GaSb oxidation, the preferential reaction of gallium with oxygen and gallium segregation at the surface is attributed to the affinity of gallium to oxygen: Ga<sub>2</sub>O<sub>3</sub> (-238 Kcal/mol) compared to antimony atoms Sb<sub>2</sub>O<sub>3</sub> (-198.2 Kcal/mol) [17]. Also, the spontaneous reaction of Sb<sub>2</sub>O<sub>3</sub> with GaSb ( $\Delta G = -12$  Kcal/mol) is attributed to the preferential reaction of gallium with oxygen in the amorphous layer [3, 18]. The exposure of GaSb to air conducted to enhance the Ga fraction at the surface [19]. In Ref. [15] are presented data concerning experimental efforts to reduce the interface defect densities ( $D_{it}$ ) to a comparable level as it is today's SiO<sub>2</sub>/Si interfaces (e.g.,  $D_{it} \sim 10^{13}$  cm<sup>2</sup>/eV, as grown) and after hydrogen passivation, this is reduced to the mid-10<sup>10</sup> range. For III-V semiconductor/oxide interfaces the lowest reported  $D_{it}$  values are in the range 10<sup>11</sup>–10<sup>12</sup> cm<sup>2</sup>/eV, and that is why the challenge in III-V compounds technology, peculiar for GaSb is to find a suitable oxide that allowed interface passivation by an appropriate passivating agent.

Most of characteristics of GaSb compound is determined by the arrangement of oxygen atoms on semiconductor surface. In GaSb Sb is octahedral coordinated by oxygen, a situation also existing in its oxygen compounds. Reaction kinetic between GaSb surface and oxygen is expressed by oxidation that takes place in two steps [3]:



Semiconductor surface structure, besides semiconductor bulk, has an important influence on the electrical properties of semiconductor devices. In this view, the study of native oxides and passivating oxides prepared in different GaSb surface oxidation procedures is necessary for the reproducibility of surface properties.

**Figure 1** shows the Ga 3*d* spectrum from the native oxides of n-GaSb(100) Te doped substrates. The lines corresponding to 18.98 and 19.50 eV are related to metallic Ga in GaSb, and the lines corresponding to 20.27 and 20.99 eV are related to Ga in Ga<sub>2</sub>O<sub>3</sub>.

The quantitative analysis indicates a percentage of 71.5% Ga in GaSb and 28.5% Ga in Ga oxide, a nonstoichiometric ratio in native oxide.

**Figure 2** shows the Sb 4*d* lines of GaSb with native oxides having the following peaks namely 32.00 and 33.27 eV for Sb in GaSb and the peaks 34.56 and 35.74 eV for Sb in Sb oxide, with an estimated composition of 71.1% Sb in GaSb and 28.8% Sb in oxide. The FWHM for Sb 4*d* lines is extended by 0.6–0.7 eV in oxide than Sb in GaSb for our experiment.

The morphological aspect of native oxide film as a conglomerate of Ga and Sb oxides defining a surface roughness of 1.854 nm is presented in **Figure 3** in an AFM image.

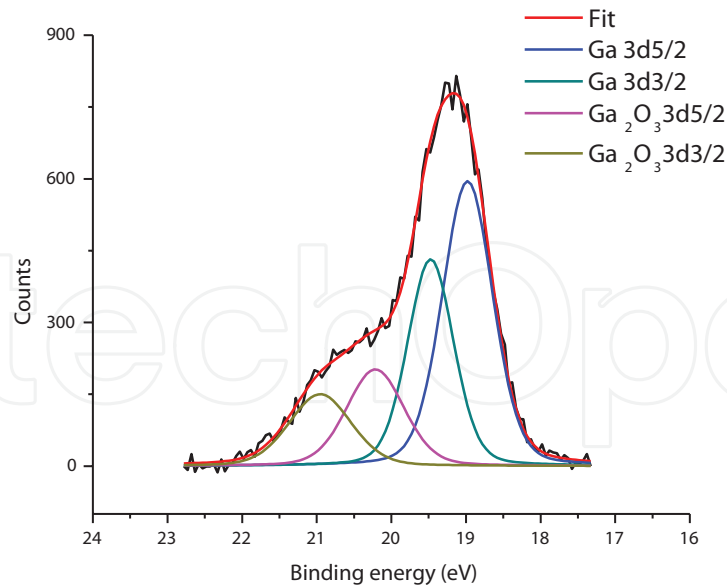


**Figure 1.** XPS spectrum for Ga  $3d$  lines on n-GaSb.

Among III-V semiconductor compounds, GaAs is probably the most studied due to its importance in modern microelectronics and optoelectronics applications. The GaAs(100) surfaces have a high surface energy [20], and the result is high reactivity and chemical unstableness. Due to the reactivity of native oxides, it is difficult to reach the passivation of GaAs surfaces. The native oxide characterization in XPS measurements led to the determination of different chemical species. The obtained data [21] indicate that the native oxide layer is complex containing amounts of carbon and oxygen. The discussions regarding surface composition are related in this work with the As  $2p^{3/2}$  and Ga  $2p^{3/2}$  signals in native oxides and subsequent changes related to different etching processes. As presented [22] the C  $1s$  peak shape has predominant contribution from C-C bond on the surface with binding energy (BE = 285 eV) that

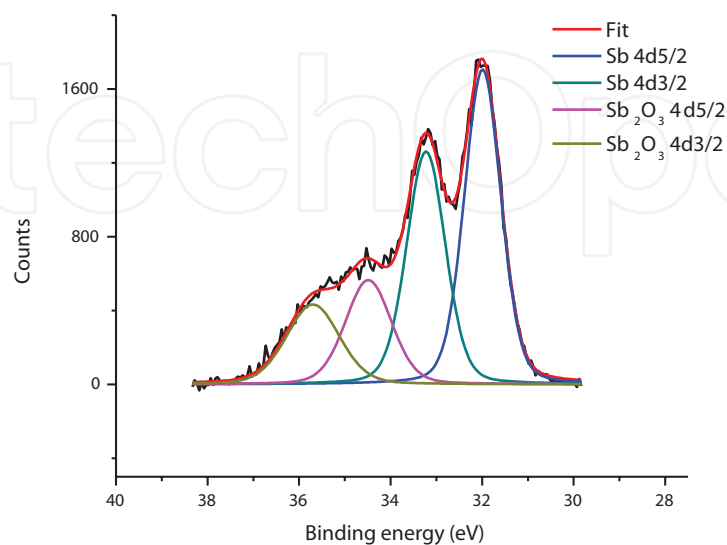


**Figure 2.** XPS spectrum for Sb  $4d$  line on n-GaSb.

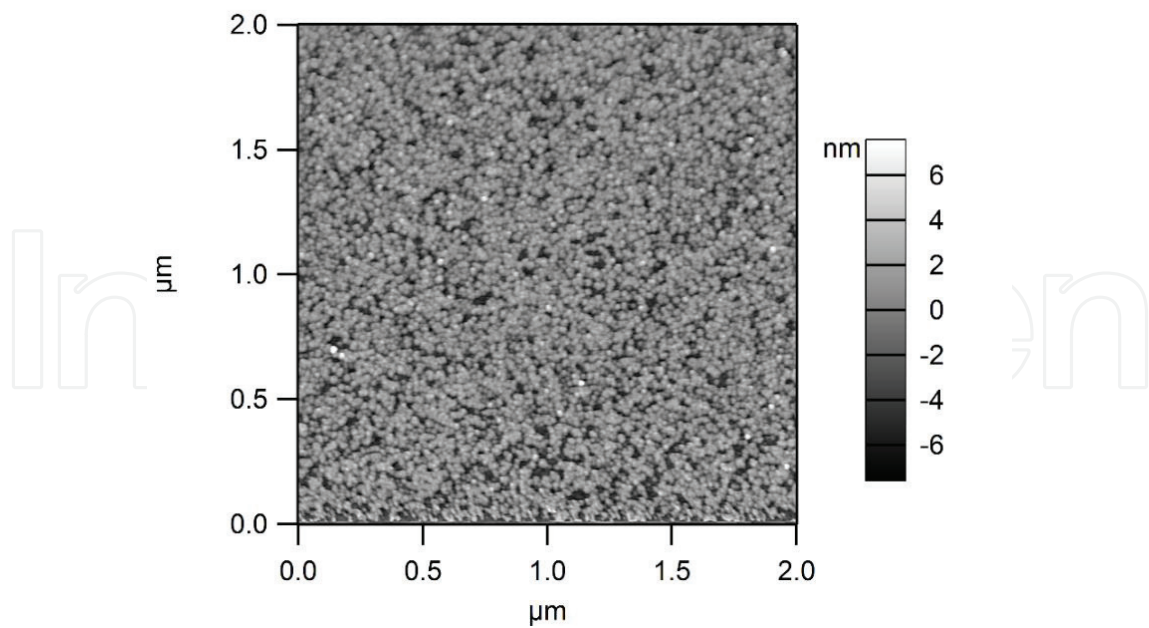


Figure 3. AFM image of GaSb covered with native oxides.

was used for BE calibration scale. The O  $1s$  is relatively broad and its main part arises from the chemisorbed oxygen at BE = 532 eV. The Ga and As  $2p$  spectra from n-GaAs(100) Te doped substrates, that contains the effect of naturally oxidized semiconductor surfaces are taken at TOA =  $90^\circ$ .

Figure 4 presents the As  $2p$  spectra from native oxides on GaAs where the line related to BE = 1323.36 eV arises from As in GaAs and the line corresponding to BE = 1326.06 eV is related to As in  $As_2O_3$ . The quantitative analysis indicates a percentage of 21.4% As in GaAs and a percentage of 78.6% that belongs to a majority of As signal from oxide ( $As_2O_3$ ).

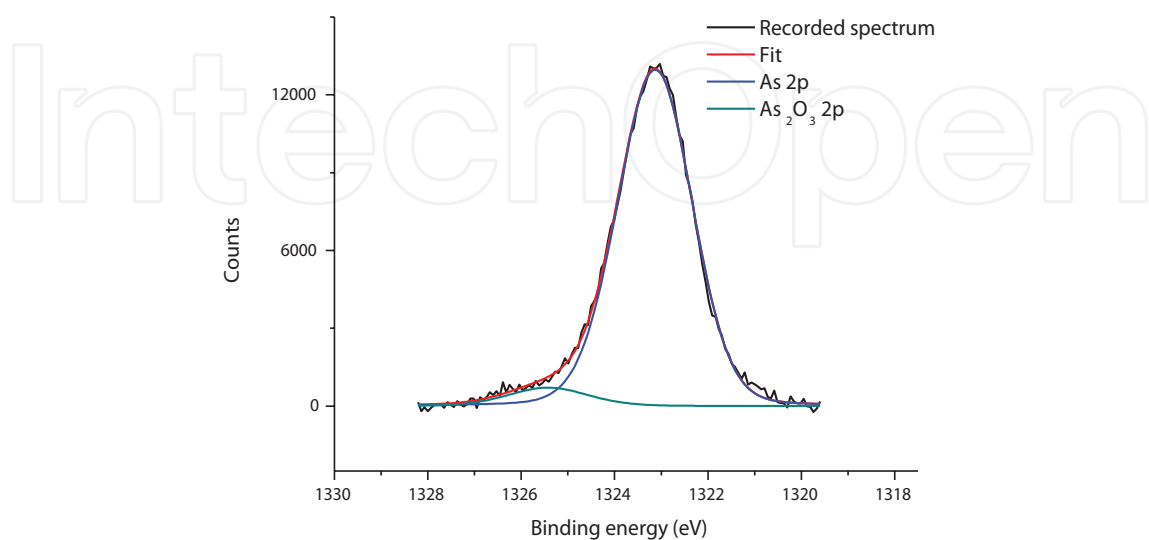
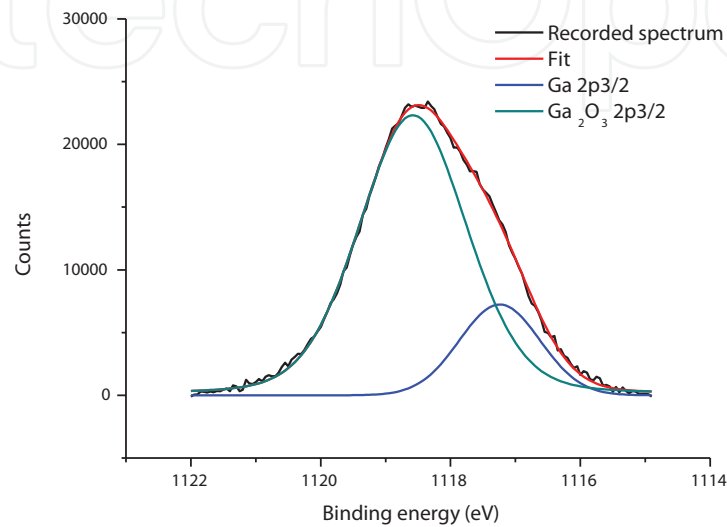


Figure 4. XPS spectra of As  $2p$  in GaAs and in  $As_2O_3$ .

**Figure 5** presents the Ga 2*p* spectra from native oxides on GaAs where the line related to BE = 1116.80 eV it arises from Ga in GaAs and the line corresponding to BE = 1118.37 eV is related to Ga in Ga<sub>2</sub>O<sub>3</sub>. The quantitative analysis indicates a percentage of 11.7% Ga in GaAs and a percentage of 88.3% that belongs to Ga in Ga<sub>2</sub>O<sub>3</sub>.

As can be observed in **Figure 6** the as-received surface of n-GaAs is covered by a conglomerate of Ga<sub>2</sub>O<sub>3</sub> and As<sub>2</sub>O<sub>3</sub>, determining on the surface a roughness characteristic of RMS ~ 0.21 nm.



**Figure 5.** XPS spectra of Ga 2*p* in GaAs and in Ga<sub>2</sub>O<sub>3</sub>.

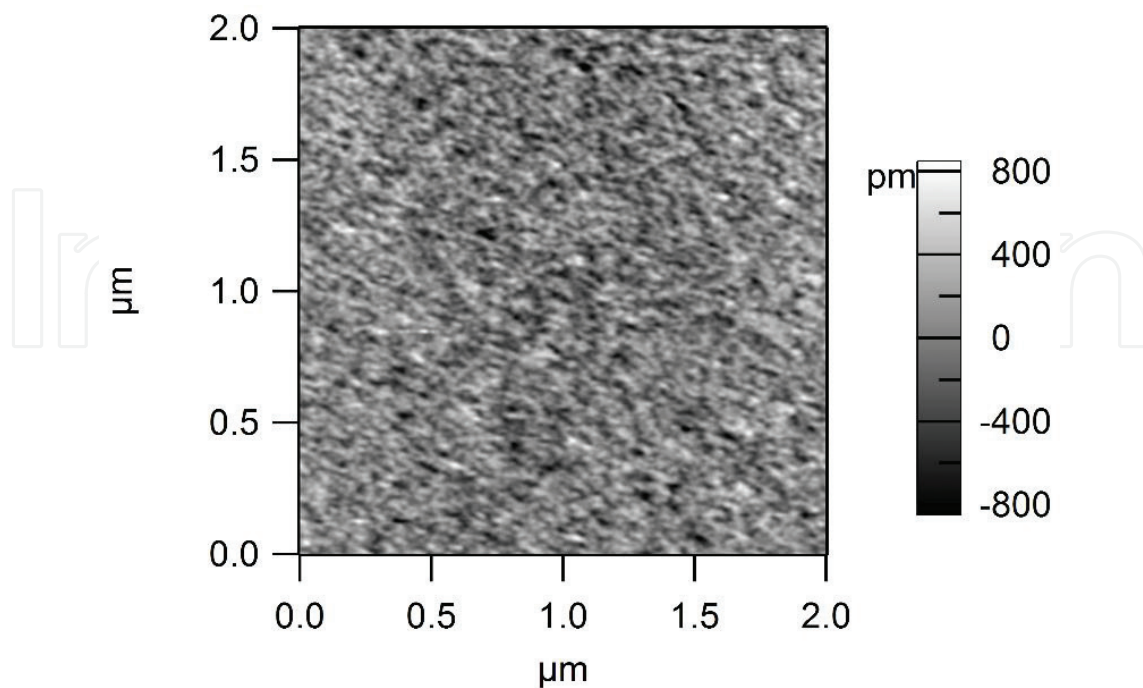


**Figure 6.** AFM image of naturally oxidized n-GaAs(100) surface.

Then n-GaP(111) native oxides structure composition were studied by XPS analysis on Ga 3d and As 2p lines where the measurements were performed at TOA = 45°. These XPS lines offer information about the presence of Gallium and Phosphorous in bulk GaP and in native oxides namely Ga<sub>2</sub>O<sub>3</sub> and P<sub>2</sub>O<sub>5</sub>. In this regard, the XPS spectra included Ga 3d<sup>5/2</sup>, 19.00 eV and Ga 3d<sup>3/2</sup>, 19.49 eV in GaP and Ga 3d<sup>5/2</sup>, 20.53 eV and Ga 3d<sup>3/2</sup>, 21.52 eV in Ga<sub>2</sub>O<sub>3</sub>. Related to P line there are present the peaks P 2p<sup>3/2</sup>, 128.63 eV and P 2p<sup>1/2</sup>, 129.58 eV arisen from GaP and P 2p<sup>3/2</sup>, 133.36 eV and P 2p<sup>1/2</sup>, 134.39 eV peaks arisen from P<sub>2</sub>O<sub>5</sub>. The XPS signals are presented for Ga 3d in **Figure 7** and for P 2p in **Figure 8**.

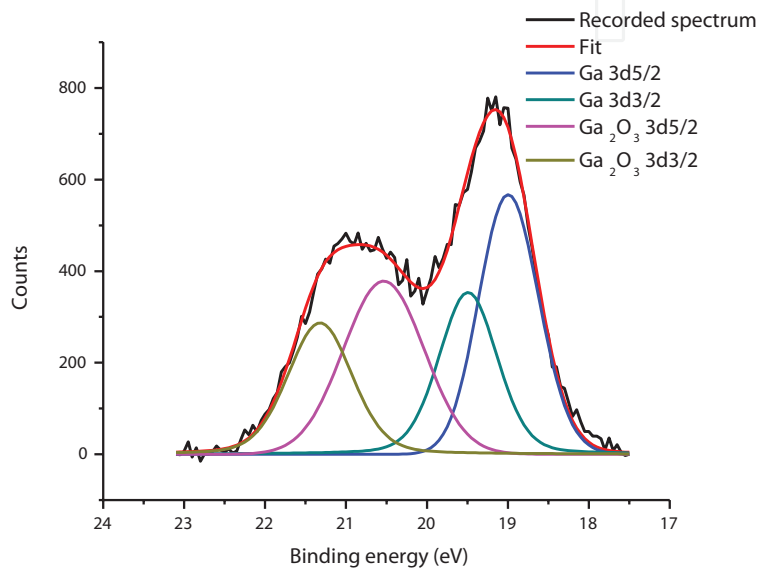


**Figure 7.** XPS spectra of Ga 3d on n-GaP(111) oxidized surface.

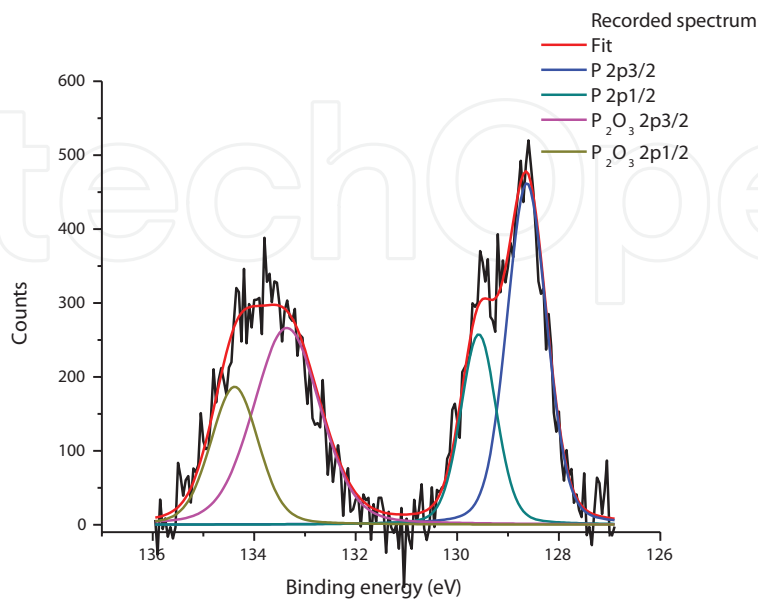


**Figure 8.** XPS spectra of P 2p on n-GaP(111) oxidized surface.



The relative composition regarding GaP surface indicated a concentration of 52.7% Ga in GaP and 47.45 Ga in  $\text{Ga}_2\text{O}_3$  and for P a percentage of 50.9% P in GaP and 49.1% P in  $\text{P}_2\text{O}_5$ . This surface structure indicates a relative balance in Ga and P, with a trend to stoichiometric value. The AFM image of GaP(111) naturally oxidized surface is presented in **Figure 10** and indicates a relative uniform distribution of  $\text{Ga}_2\text{O}_3$  and  $\text{P}_2\text{O}_5$ .

The AFM image from **Figure 9** for n-GaP(111) surface indicates the existence of a conglomerate of  $\text{Ga}_2\text{O}_3$  and  $\text{P}_2\text{O}_5$  that determines on the surface roughness characteristic of RMS  $\sim 4.54$  nm.

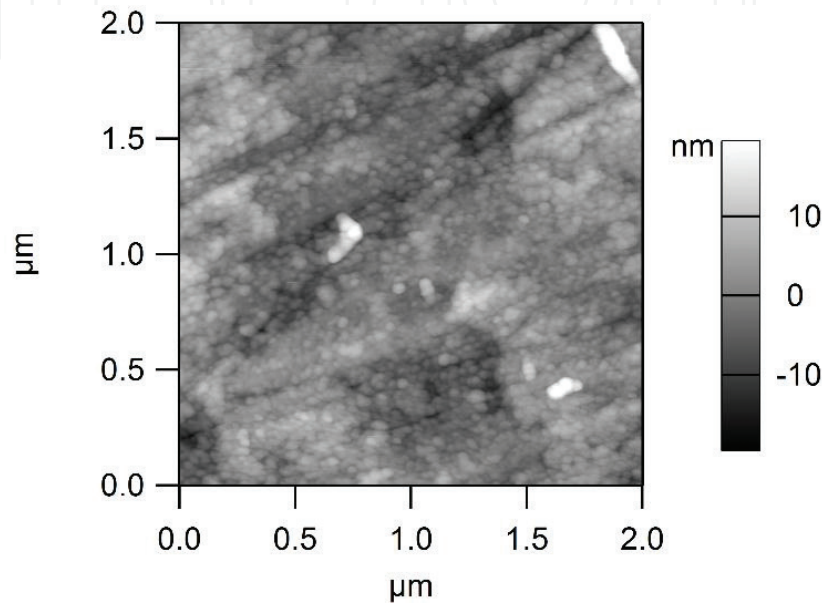


**Figure 9.** AFM image of naturally oxidized n-GaP(111) surface.

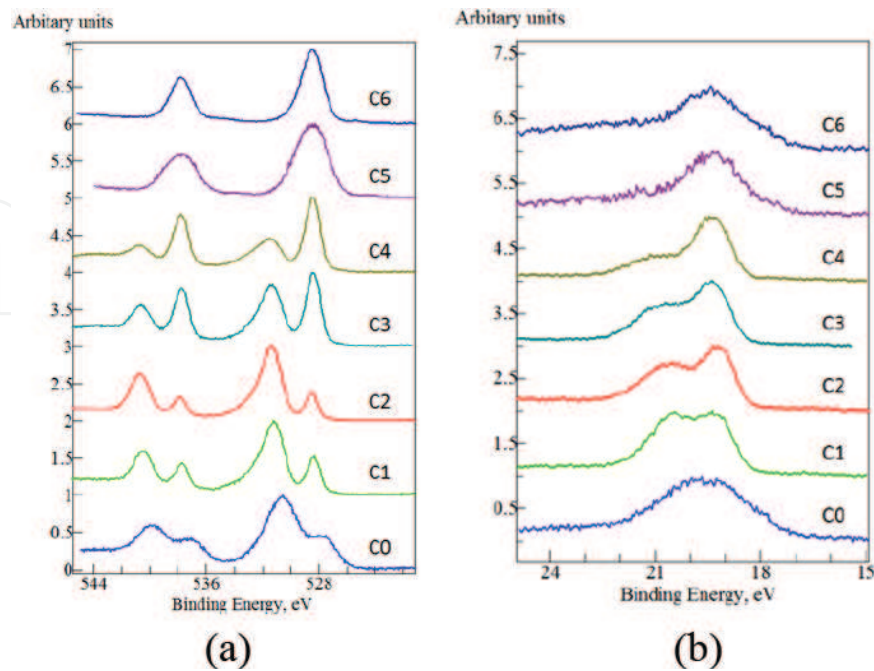


**Figure 10.** Superposition of XPS spectra for Sb 3d (a) and Ga 3d (b) at TOA:  $90^\circ$  (C0- sample as received; C1, C2, C3, C4, C5, C6).

## 4. Surface modification

As it was stated in Ref. [23], the implementation of GaSb-based alloys in device technology is depended on reproducible control of their surface properties. In this view, the real GaSb surfaces are modified by technological processes namely cutting, smoothing, or mechanical polishing of semiconductor wafer a fact that conducted to surface damage regions. Compared to GaAs or InP, the GaSb surface is more reactive and GaSb surface oxidized rapidly in ambient conditions and the resulted oxide layer is not self-limiting, stable nor abrupt [24]. Chemical reactivity of antimonides present them as a distinct category of materials [25]. The irreversibility character of the reactions implies that oxygen atoms, rather than molecules are ultimately involved in chemical bonding. It is important to note [23] that for oxygen involved there is a movement from the chemisorption concept (i.e., adsorbed layer structure is a function of underlying surface) to the complex formation concept characterized by a film with its own chemical and structural identity. Generally speaking the different structure of III-V semiconductor surface determined a basic influence on the surface electrical properties. This influence manifest itself by the generation of electronic states (i.e., surface and resonant states) that induced the Fermi level pinning on semiconductor surface. Fermi level pinning may conducted to density of surface states in the order  $10^{12} \div 10^{13} \text{ cm}^{-2}$ . Chemisorption and chemical reactions may conducted to a modification of surface states and to the generation of new donor and acceptor states in the band gap. Study of the preparation methods of semiconductor surfaces in order to obtain a surface with characteristic as: free of damage, contamination, and native oxides is essential for reproducible and efficient control of surface properties. It is observed [23] that in device technology practice contact with atmosphere is unavoidable and surface preparation usually takes place by etching processes. The surface of n-GaSb(100) Te doped is generally chemical prepared by a cleaning procedure in organic solvents, e.g., trichloroethylene, acetone, and afterwards is chemical etched HF:H<sub>2</sub>O (DIW) (1:1) for 15 seconds, and HCl:H<sub>2</sub>O(DIW) (1:1) for 15 seconds and then rinsed in DIW. In the following will be presented the effect of chemical etching in a mixture of HCl:H<sub>2</sub>O(DIW):C<sub>6</sub>H<sub>8</sub>O<sub>7</sub> (citric acid), after an exposer at room temperature for an etching time in the range 35 ÷ 300 seconds. The evolution of native oxides was put into evidence by a XPS analysis at TOA = 90°, as is presented in **Figure 10**. It can be observed that the Sb signal from GaSb is increasing and the signal from oxide is decreasing (91.5 to 8.5% in composition table) and the signal from Ga in GaSb has a higher intensity as the O line in Ga oxide. This effect is a consequence of the surface chemical etching and to the fact that for this solution the Sb oxide and Ga oxide are both sensitive that is why this etchant can be used further in technology for a rapid cleaning of the n-GaSb(100) surface. The evolution of Sb native oxides and Ga native oxides on n-GaSb(100) as a result of chemical etching can be seen in the superposition presented in **Figure 10(a)** for Sb 3*d* spectra in different stages of etching namely: C1 (*t*<sub>1</sub> ~ 30–35 seconds); C2 (*t*<sub>2</sub> ~ 65 seconds); C3 (*t*<sub>3</sub> ~ 90 seconds); C4 (*t*<sub>4</sub> ~ 120 seconds); C5 (*t*<sub>5</sub> ~ 180 seconds); C6 (*t*<sub>6</sub> ~ 300 seconds); (b) for Ga 3*d* spectra in the same chemical etching stages. The signal arising from Ga 3*d* shows the same trend for Ga oxides, the surface Ga oxides are removed after C5, which means that both Sb and Ga oxides had the same behavior, and the sample is prepared in these conditions of chemical etching for further processing.

**Figure 11** presents the AFM image of n-GaSb(100) surface after 90 seconds of chemical etching. As can be observed there is a strong attack of the etching solution at the surface where the network aspect is characterized by valleys and hills and the roughness is high, i.e., RMS ~ 13.96 nm.

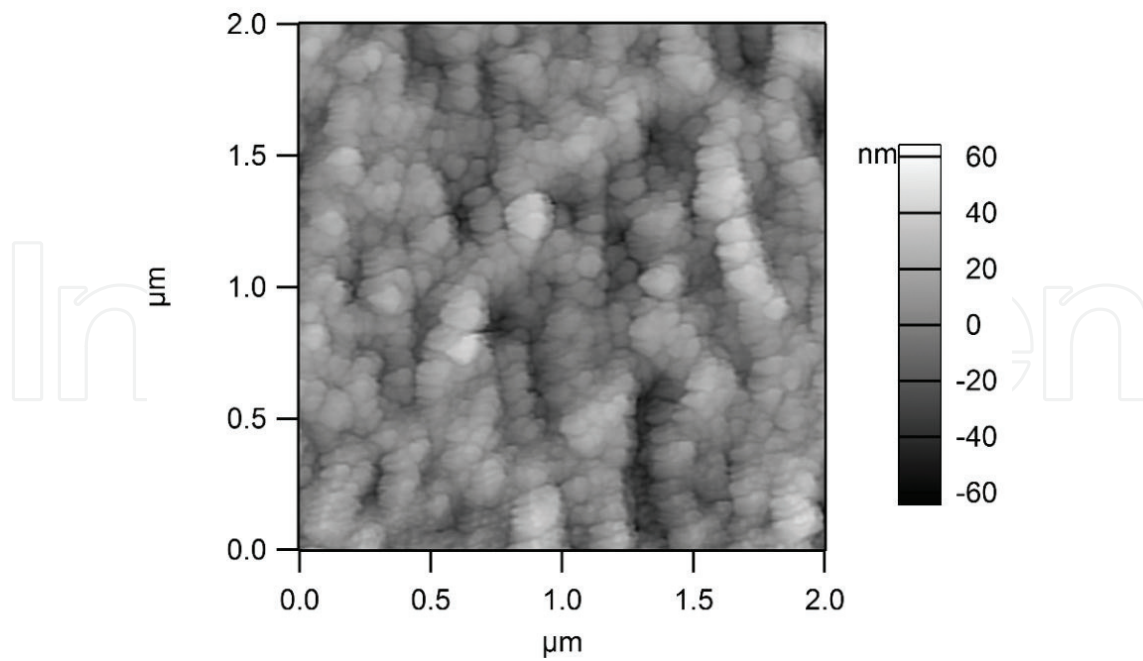


**Figure 11.** AFM image of n-GaSb(100) after 90-second chemical etching.

The effect of  $\text{Ar}^+$  ion etching on n-GaSb native oxides for different voltages and etching times can be observed from XPS spectra, i.e., C1 (0.5 kV,  $t_1 = 3$  minutes); C2 (1 kV,  $t_2 = 3$  minutes); C3 (1 kV,  $t_3 = 5$  minutes); C4 (2 kV,  $t_4 = 10$  minutes). **Figure 12** presents the XPS signal for a TOA =  $20^\circ$  for Sb 4d line, a signal sensitive to the surface composition.

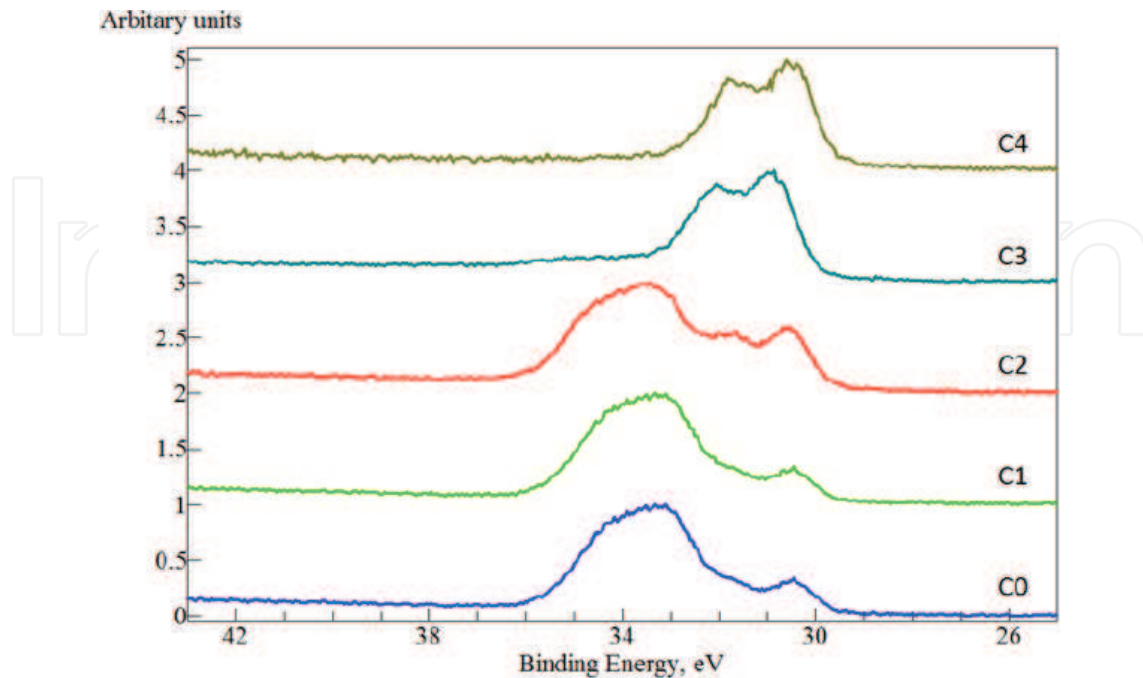


**Figure 12.** The evolution of Sb oxide after ion etching for Sb 4d signal C0- as received, C1, C2, C3, C4).

The signal for antimonide oxides present on the as-received sample (a sample covered with native oxides) starts to modify its intensity during etching process, and at the last Ar<sup>+</sup> etching (C4) it remains only the signal from Sb 4d in the bulk of GaSb (~35 eV, ~32 eV). In the evolution of native oxides on GaSb during Ar<sup>+</sup> ion etching can be observed that the Sb oxides are the first one to be cleared off, and then are cleared off Ga oxides [26]. As the result of an ion beam cleaning process, the native oxides vanishes, e.g., Ga oxides signals are the first ones with a decreasing intensity until Ga 3d signal from Ga<sub>2</sub>O<sub>3</sub> disappears after C4 ion etching.

The effect surface passivation by chemical reaction on n-GaSb(100) with sulfur compounds (e.g., S<sub>2</sub>Cl<sub>2</sub> and (NH<sub>4</sub>)<sub>2</sub>S) is presented in **Figure 13** as an AFM image.

Passivation by S<sub>2</sub>Cl<sub>2</sub> chemical reaction and the presence of GaSb-S thin films exhibited moderate to high toxicity against gram-positive bacterial strain (*Staphylococcus aureus*), demonstrated by the formation of a clear inhabitation zone around the coated substrate. The presence of sulfur bond is putted into evidence by the S 2s XPS as recorded signal observed in **Figure 14**.

We consider that the passivated n-GaSb studies open a gate for a possible active biological GaSb device obtained on a sulfur-passivated surface in a compatible technology of III-V compounds.

A real GaAs surface is covered with a relatively thick layer (a few nanometers) of native oxide, which is the origin of a high density of surface states  $N_{ss} \sim 10^{12} \text{ cm}^{-2}$  (under technological conditions) pinning the surface Fermi level within the band gap of the semiconductor. In the case of GaAs, as it was mentioned in Ref. [20], the GaAs(100) surfaces have a high surface energy and as a consequence they are very reactive and chemically unstable. Regarding the

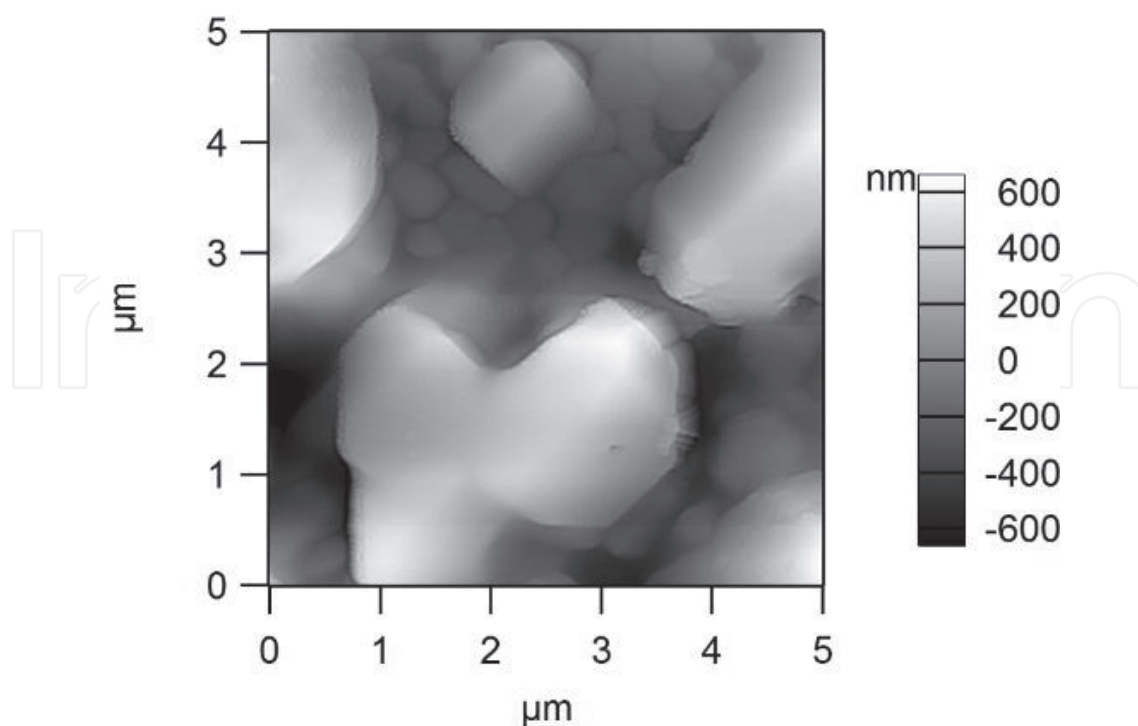


**Figure 13.** Aspect of n-GaSb(100) surface exposed to S<sub>2</sub>Cl<sub>2</sub> action.

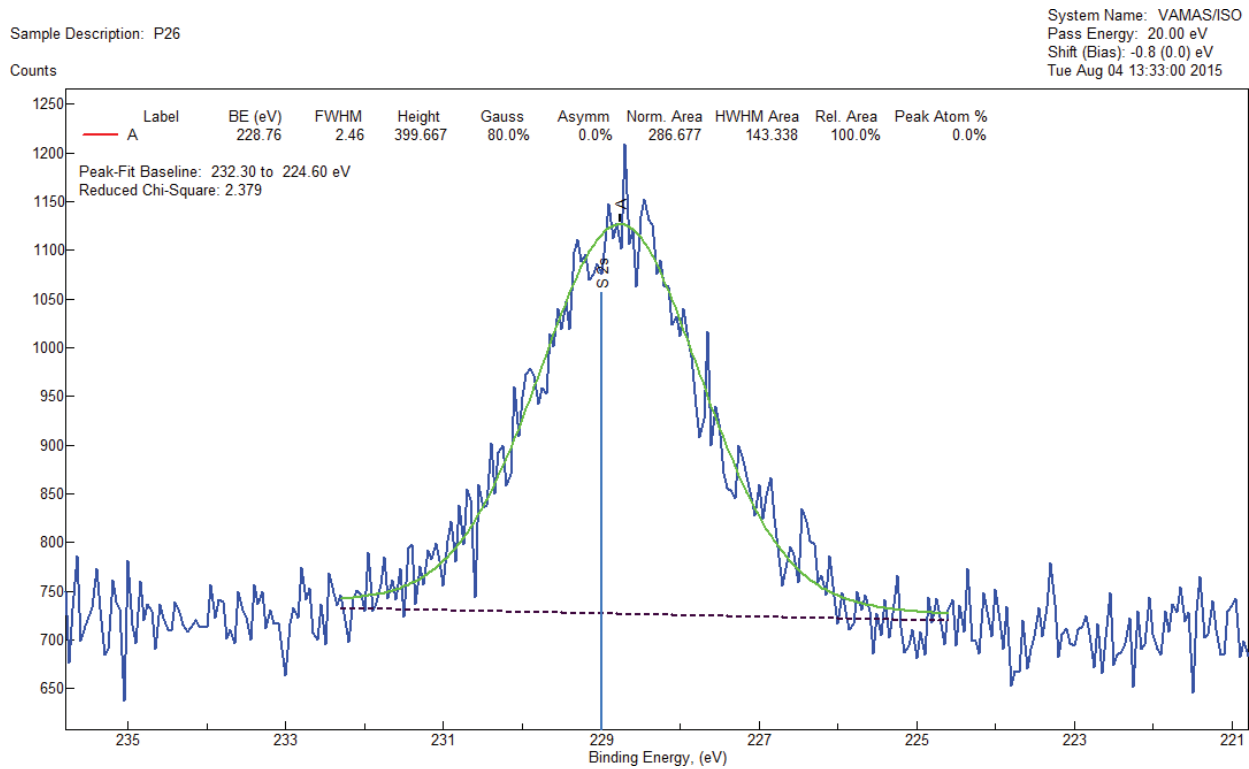


**Figure 14.** XPS recorded signal for S 2s line (linked to Sb) on n-GaSb passivated by  $S_2Cl_2$ .

surface analysis of GaAs native oxides in the case of XPS measurements there exist a great dispersion of XPS values [27]. In the perspective of native oxides reactivity, it is worth to understand that it is difficult to reach the passivation of GaAs surfaces. The aim of surface passivation is to reduce the surface state density, or preferably, to remove them from the band gap. The surface of n-GaAs(100) Te doped was prepared by a cleaning procedure at room temperature in organic solvents, i.e., trichloroethylene, acetone, and afterward it is generally chemical etched in  $HCl:H_2O_2$  (1:1) for 30 seconds and then rinsed in DIW or chemical etched in  $H_2SO_4:H_2O_2:H_2O$  (DIW) (1:1:1) for maximum 5 minutes and then rinsed in DIW. The As 2p XPS signal from the chemical etched n-GaAs(100) is observed in **Figure 15**. The signal derived from As in  $As_2O_3$  after the chemical cleaning procedure is close to the background, a fact that suggested that the native oxide was removed. The same conclusion derived from the XPS Ga 2p signal from the chemical-etched GaAs(100) is observed in **Figure 16**. The Ga line from  $Ga_2O_3$  after cleaning procedure is close to the background as a result of native oxide removal.

A variant of n-GaAs(100) surface preparation is the sulfur passivation by organic and inorganic compounds. The sulfur treatment of the GaAs surface in sulfide solutions results in the removal of the native oxide layer and the formation of As-S and Ga-S covalent bonds [28], where the processes are accompanied by a marked reduction of surface recombination velocity.

In this perspective in the case of GaAs the chemical treatment by sulfur tend to minimize the values of  $N_{ss}$  and  $v_s$  (surface recombination velocity)  $\sim 10^7$   $cm s^{-1}$ . From a chemical point of view sulfur passivation involves a removal of native oxide layer and the formation of thin protective layer on n-GaAs in order to prevent its oxidation in atmosphere. From the electrical

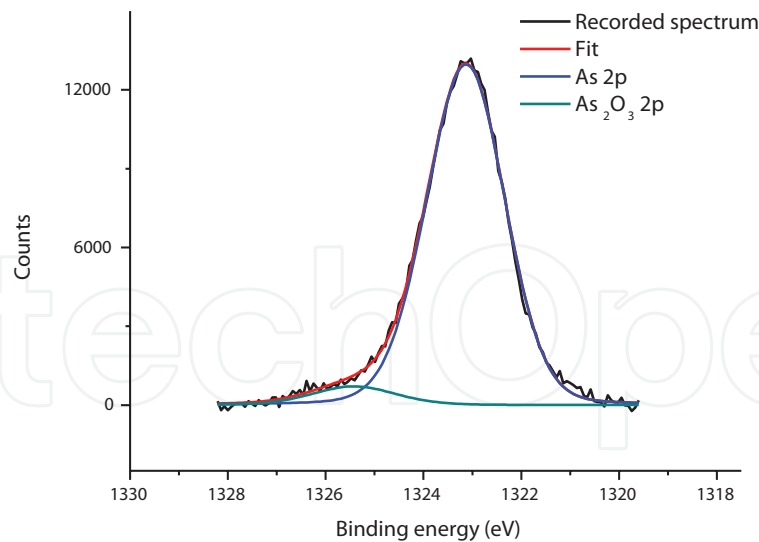


**Figure 15.** As 2*p* XPS spectra from n-GaAs chemical etched surface.

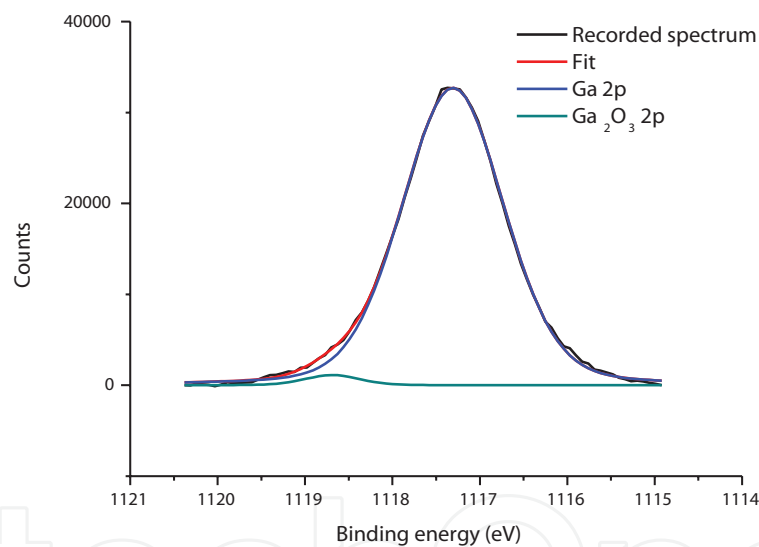


**Figure 16.** Ga 2*p* XPS spectra from n-GaAs chemical etched surface.

point of view the passivation is related as was stated before with the reduction of surface state density and as a consequence is the change of surface potential barrier on GaAs. Prior to sulfur treatment the wafers were degreased in trichloroethylene (boiling for 2 minutes), rinsing in acetone and then chemical etched in HCl:H<sub>2</sub>O (DIW) (1:1) for 100 seconds at room temperature. The n-GaAs wafers presented the aspect of an optical polished surface. The sulfide treatment was carried out in two different solutions namely: (a) pure ammonium sulfide (NH<sub>4</sub>)<sub>2</sub>S (50% H<sub>2</sub>O)—as stated an aqueous solution and (b) solution of sulfur monochloride (S<sub>2</sub>Cl<sub>2</sub>) in carbon tetrachloride (CCl<sub>4</sub>) (1:10). The SEM micrograph on sulfur-treated n-GaAs(100) revealed a uniform deposition of sulfur compounds (S<sub>2</sub>Cl<sub>2</sub> and (NH<sub>4</sub>)<sub>2</sub>S) on different regions on the sample area of over 1 cm<sup>2</sup> as presented in **Figure 17(a, b)**.

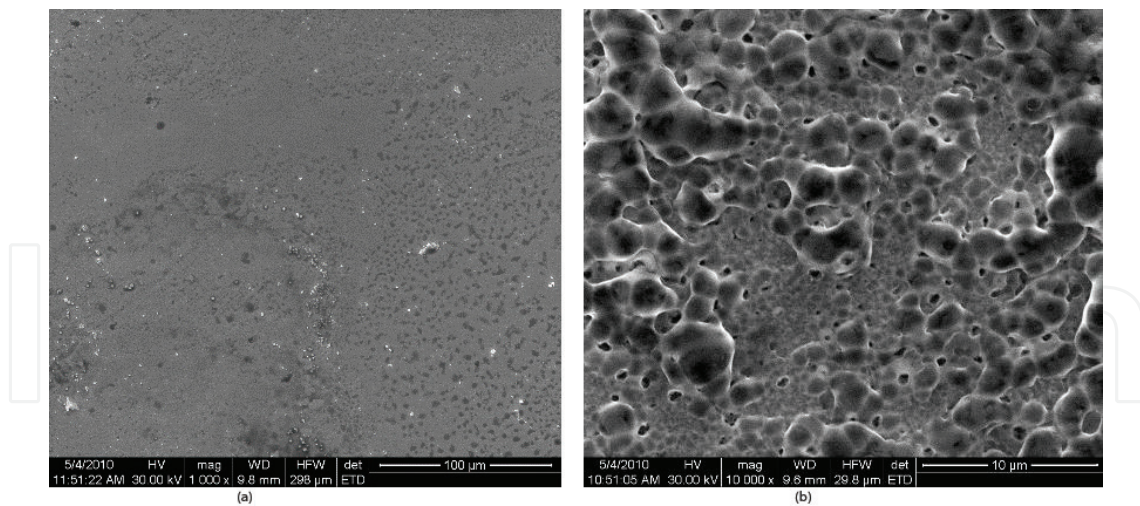


**Figure 17.** SEM images for (a)  $S_2Cl_2$  and (b)  $(NH_4)_2S$  deposition on n-GaAs(100).

In the followings, we present the results of a more complex procedure for n-GaAs(100) cleaning, namely combined chemical etching with controlled thermal treatment. The as-received GaAs wafers were firstly chemical etched in  $HCl:H_2O_2$  (1:1) for 30 seconds and rinsed in  $H_2O$  (DIW) and afterwards exposed to thermal treatment at  $200^\circ C$  for  $t = 1$  h in high vacuum ( $p \sim 10^{-9}$  torr). The XPS spectra of the as-prepared GaAs(100) surface recorded for As 2p and Ga 2p lines are presented in **Figure 18(a, b)**.

As can be observed the XPS signals for As and Ga in native oxides vanish and the only signals present are the ones for As and Ga in GaAs. The XPS extracted information indicate that the combined cleaning procedure used is effective, the n-GaAs(100) is prepared for further technological stages. Another possibility for preparing n-GaAs(100) surface is the cleaning by physical means, namely sputtering technique. The experiment of  $Ar^+$  ion beam etching implied an accelerating voltage of  $U = 500$  V, for medium time interval of 100 seconds.

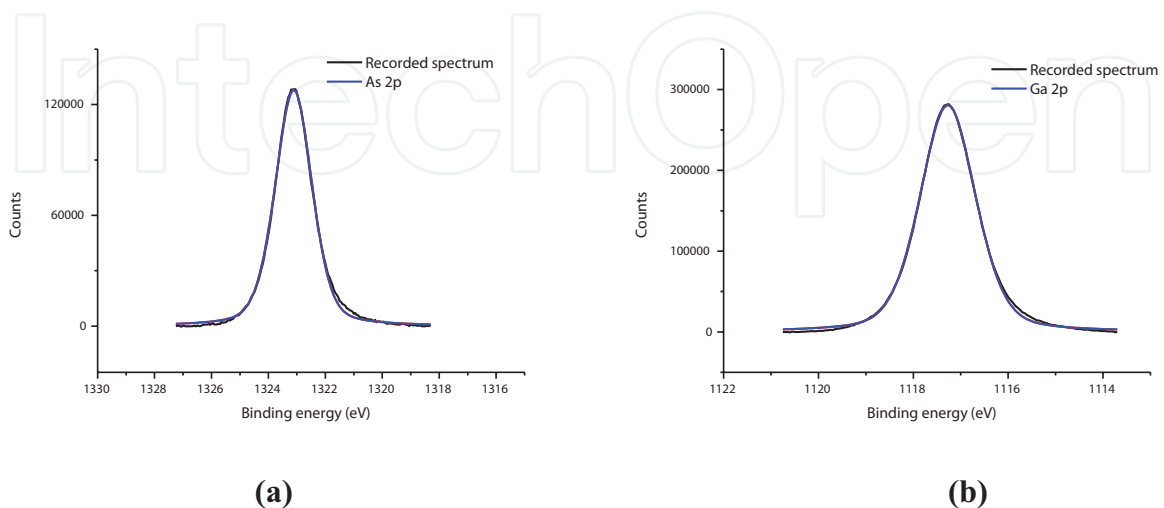


**Figure 18.** XPS spectra for (a) As 2p and (b) Ga 2p for a complex treatment of n-GaAs(100) surface.

The result of the as-prepared n-GaAs(100) surface indicates that the ion beam etching is effective in cleaning the GaAs native oxides, but the exposed surface is damaged by ion beam. This damaging effect is observed in the XPS spectra for As 3*d* and Ga 3*d* line as an enlargement of main peak (FWHM-Full Width at Half Maximum). In **Figure 19(a, b)** can be observed the absence of As and Ga signals from native oxides (As<sub>2</sub>O<sub>3</sub>, Ga<sub>2</sub>O<sub>3</sub>), that indicated the presence of a cleaned surface, together with an enlarged signals of As and Ga arisen from GaAs ion damaged surface.

The naturally oxidized n-GaP(111) samples were cleaned by chemical etching in a solution of H<sub>2</sub>SO<sub>4</sub>:H<sub>2</sub>O<sub>2</sub>:H<sub>2</sub>O (DIW) (3:1:1) for *t* = 5 minutes at a temperature of *T* ~ 39°C and then rinsed in DIW. As it has been observed in Ref. [8], the P/Ga atomic ratio on the semiconductor surface has a near stoichiometric value. For a complete preparation of GaP surface in order to be exposed to further technological procedures, the chemical etched wafer was exposed to a thermal treatment at about *T* = 200°C for a time range *t* = 2 h in high vacuum (*p* ~ 10<sup>-9</sup>) torr conditions. The cleaning effect of chemical-thermal treatment can be observed in the Ga 3*d* and P 2*p* XPS surface recorded spectra as they are presented in **Figure 20**. The effect of surface

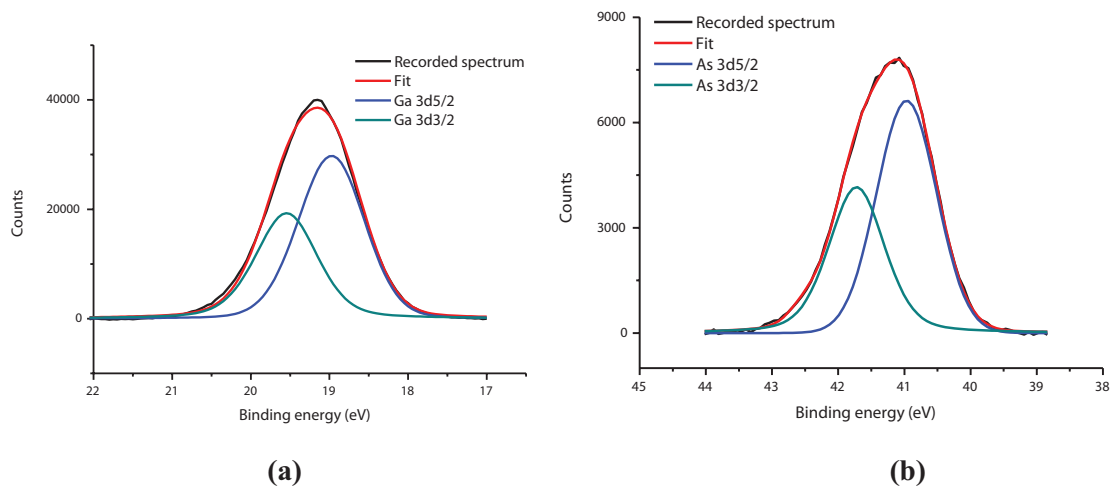


**Figure 19.** XPS spectra of (a) Ga 3*d* and (b) As 3*d* lines on an ion beam etched n-GaAs(100) surface.

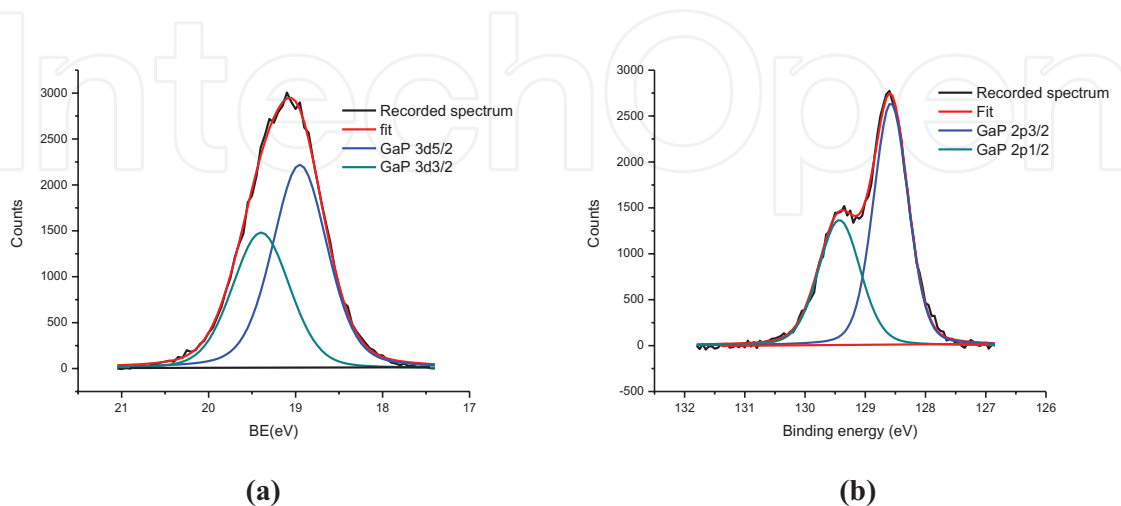


**Figure 20.** XPS spectra of (a) Ga 3*d* and (b) P 2*p* for as-prepared n-GaP(111) surface.



preparation is characterized firstly by the vanishing of native oxide signals ( $\text{Ga}_2\text{O}_3$  and  $\text{P}_2\text{O}_5$ ) and secondly by the spectral line characteristics of a FWHM  $\sim 0.8$  eV that indicates a well reconstructed surface without surface damages and with a Ga/P  $\sim 1$  ratio, that means a stoichiometric aspect. The simple GaP wet chemical etching can remove the native oxide layer but as soon as the sample is exposed to air, the wafer is again naturally oxidized.

The  $\text{Ar}^+$  ion sputtering GaP prepared surface, in the energy limit of  $1 \div 5$  keV and sputter time  $t = 5$  minutes, indicates [8] a decrease of the XPS signal arising from oxides. The oxide overlayer was removed by sputtering and the changes in both core-level signals of Ga and P indicate that sputtering process causes P depletion in n-GaP surface. The  $\text{Ar}^+$  ion bombardment generates a near-surface layer depleted of “volatile atoms” ( $\text{Ar}^+$  sputter rates for GaP, GaAs are relatively low, i.e.,  $<250$  nm/min [29]) and the compositional changes generated by preferential sputtering is propagating into bulk by diffusion processes. In this view, the distribution of Ga and P atoms in outer layers can be explained by the competition between preferential sputtering of P versus Ga and radiation-enhanced surface diffusion Gibbson segregation by the analogy with the distribution mechanism for Ga and As [30, 31]. Due to the preferential sputtering, the resulted surface composition is considerably different from the stoichiometric bulk composition and the observed depletion of P species from the surface is related to a sublimation energy of P smaller than of Ga [30]. This preferential sputtering of P and  $\text{P}_2\text{O}_5$  in the outer layer is responsible for the increase of Ga/P ratio to 1.5 and in consequence to a surface enrichment in Ga atoms. The  $\text{Ar}^+$  ion sputtering of n-GaP(111) surface is efficient in removing the native oxides, but the remaining etched surface is intensely nonstoichiometric and the reconstruction procedure is more complicated.

## 5. Aspects of metal deposition on prepared surface of III-V compounds

As it was presented, gallium antimonide (GaSb) is of special interest as a substrate material for device applications as laser diodes with low threshold voltage, photodetectors with high efficiency, high frequency devices, or high efficiency thermophotovoltaic (TPV) cells. Fabrication of PV discrete devices generally begins with defining the active structure by a Schottky photosensitive contact or the growth of MBE (molecular beam epitaxy) heteroepitaxial layers. One of the most important parts of fabrication procedure is obtaining low resistivity ohmic contacts on broad area of photosensitive surface in order to realize a competitive serial resistance ( $R_s$ ). For a PV device, a good  $R_s$  assures an optimal fill factor (ff) related to an extended spectral response of photocurrent ( $I_{\text{ph}}$ ). The problems connected to the formation of ohmic contacts on p- or n-GaSb represent a technological skill considered in general a real state-of-art in obtaining semiconductor devices [3]. The investigation of the characteristics for low resistance Au/Ge/Ni nanometric contact layers deposited on n-GaSb(100) is a part of a general technological effort in order to define conditions for obtaining a PV competitive device. The Au/Ge/Ni with characteristic, i.e., Au (139 nm)/Ge (72 nm)/Ni (14 nm), contact layers were deposited in medium vacuum ( $p \sim 8 \times 10^{-5}$  torr) and then annealed in low vacuum ( $p \sim 7 \times 10^{-2}$  torr) low temperature ( $T \sim 300^\circ\text{C}$ ) for  $t = 3$  minutes. In this contact technology, the role of Au is to facilitate Ga diffusion from the surface, the role of Ge is to occupy the Ga vacancies

in GaSb and to dope the first semiconductor layers in a  $n^+$  fashion, the consequence being the decrease the ohmic characteristic for the contact. In this conjuncture the Ni part is to assure the wettability of the contact and the thermal stability [32]. In order to analyze the as-mentioned characteristics of Au/Ge/Ni deposition the depth profiling measurement of AuGeNi contact was obtained in SPECS system by XPS analysis after controlled plasma etching ( $\text{Ar}^+$  ions at energy  $E = 3 \text{ KeV}$ , pressure  $p \sim 10^{-5} \text{ torr}$ , ion current  $I_{ic} = 10 \mu\text{A}$ ). In **Figure 21(a-c)**, the as-recorded...” is appropriate.

**Figure 21(a-c)**, the as-recorded XPS spectra for Au  $4f$ , Ge  $2p$ , and Ni  $2p$  arisen from the initial metal deposition n-GaSb surface are presented.

The effect of  $\text{Ar}^+$  ion beam sputtering in the experiment of depth profiling can be observed in **Figure 22(a-c)** from the XPS recorded after the 16th controlled etching.

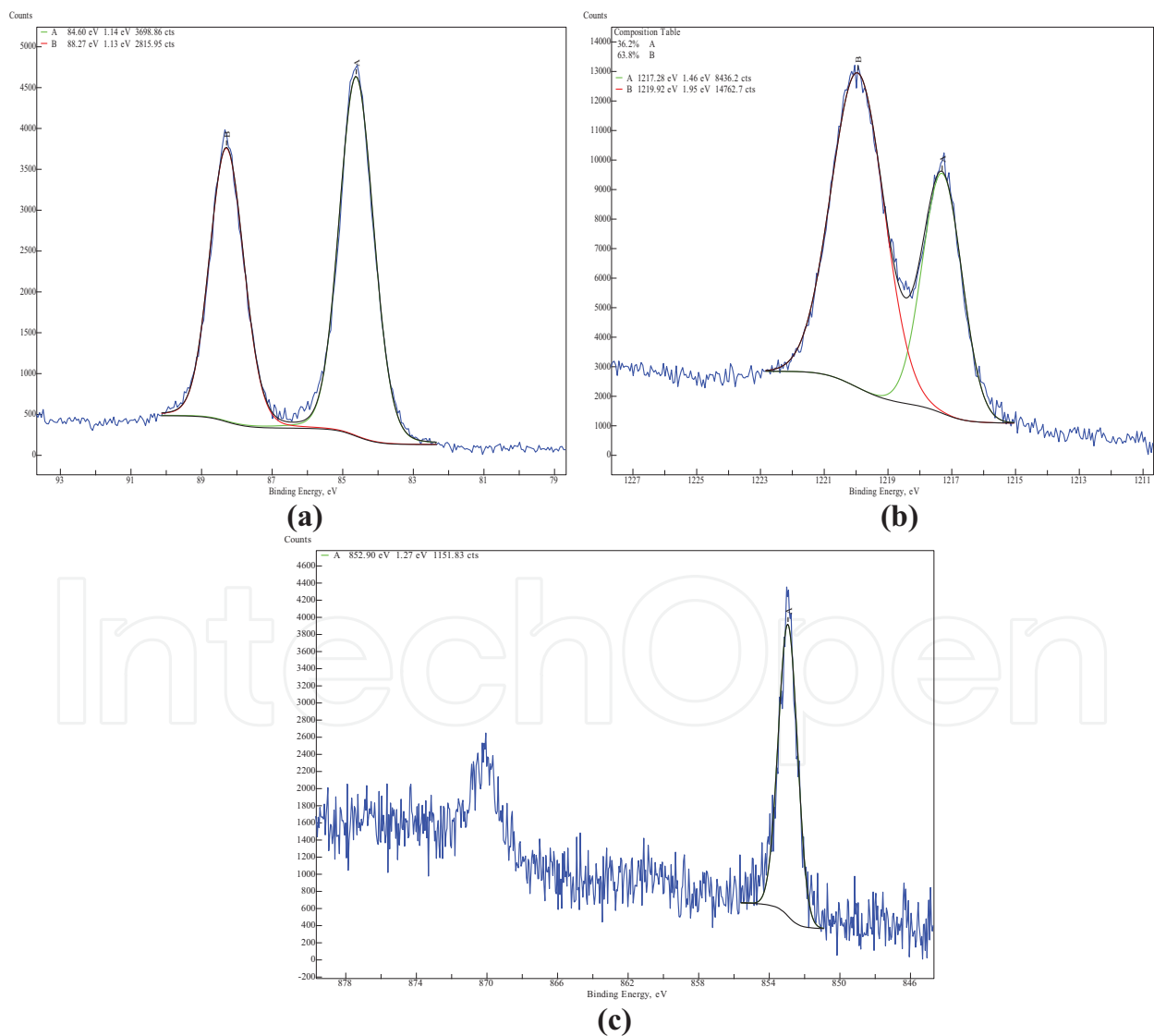


**Figure 21.** XPS spectra of (a) Au  $4f$ , (b) Ge  $2p$ , and (c) Ni  $2p$  deposited on n-GaSb(100).

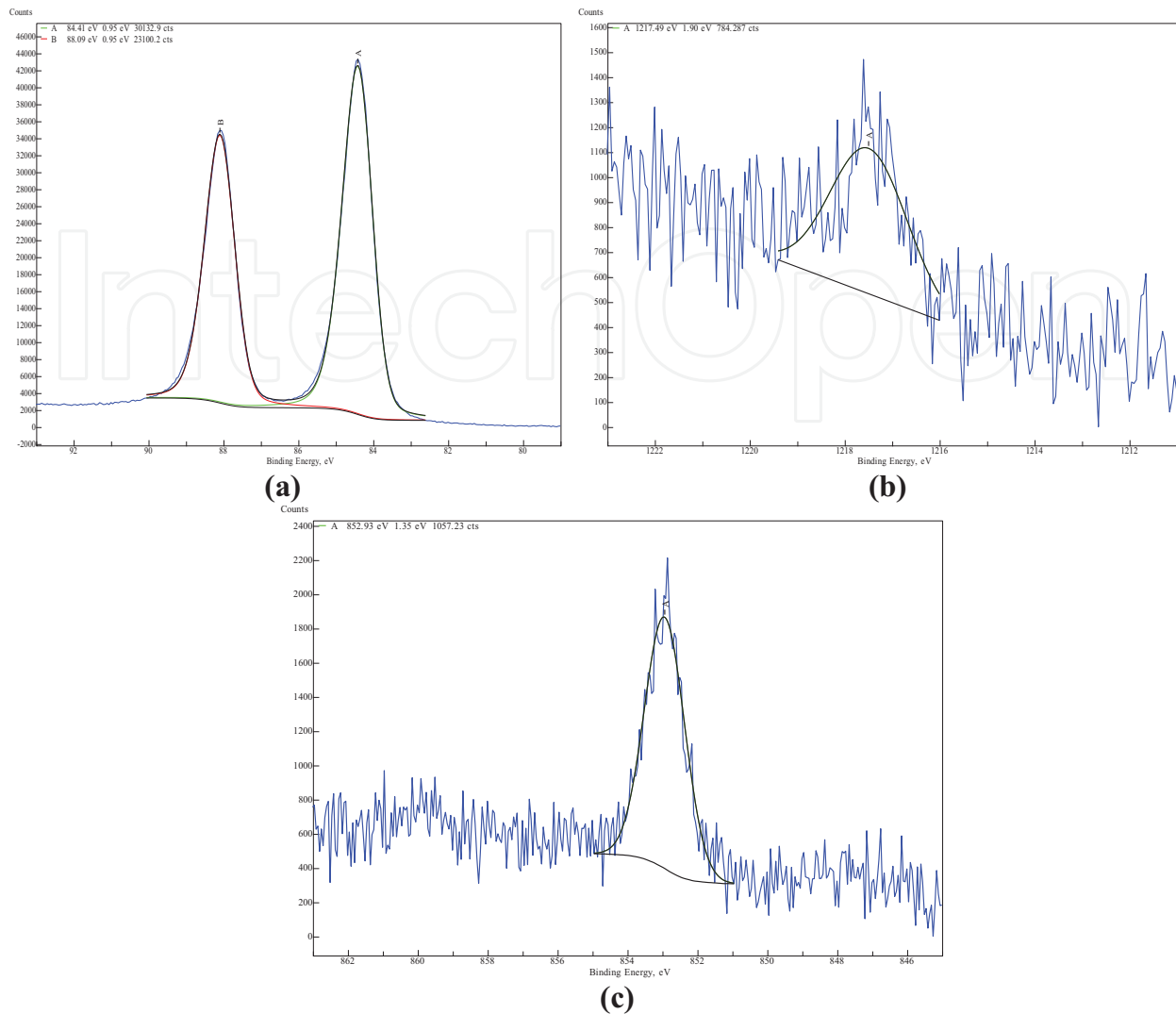


**Figure 22.** XPS spectra of (a) Au 4*f*, (b) Ge 2*p*, and (c) Ni 2*p* after 16th ion beam etching.

The AFM aspect of the AuGeNi surface after controlled ion beam etched can be observed in **Figure 23**.

The elemental composition of the sample namely AuGeNi/n-GaSb was also investigated by Rutherford Backscattering Spectrometry (RBS), as a surface sensitive analysis technique. The depth profiles of the elements contained in the deposited contact layer are presented in **Figure 24**. The scattering profile of Au appear at an energy of 2769 keV. The thickness was determined to be  $1500 \times 10^{15}$  at/cm<sup>2</sup>. The concentration of Au is increasing from 30 at. % to 70 at. % from the surface to a depth of  $500 \times 10^{15}$  at/cm<sup>2</sup>. The depth profile of Ge is rather similar. The concentration of Ge is also increasing from 15 at. % to 30 at. % from the surface to a depth of  $500 \times 10^{15}$  at/cm<sup>2</sup>. Ni was present only in the first  $500 \times 10^{15}$  at/cm<sup>2</sup> part of the layer, with a decreasing concentration starting from 55 down to 15 at. %.

The initial defining of AuGeNi as an ohmic contact on n-GaSb can be remarked in **Figure 25** presenting the I-V characteristics of a MBE Ni/GaSb Schottky diode (Ni contact thickness  $\sim 2$  nm).

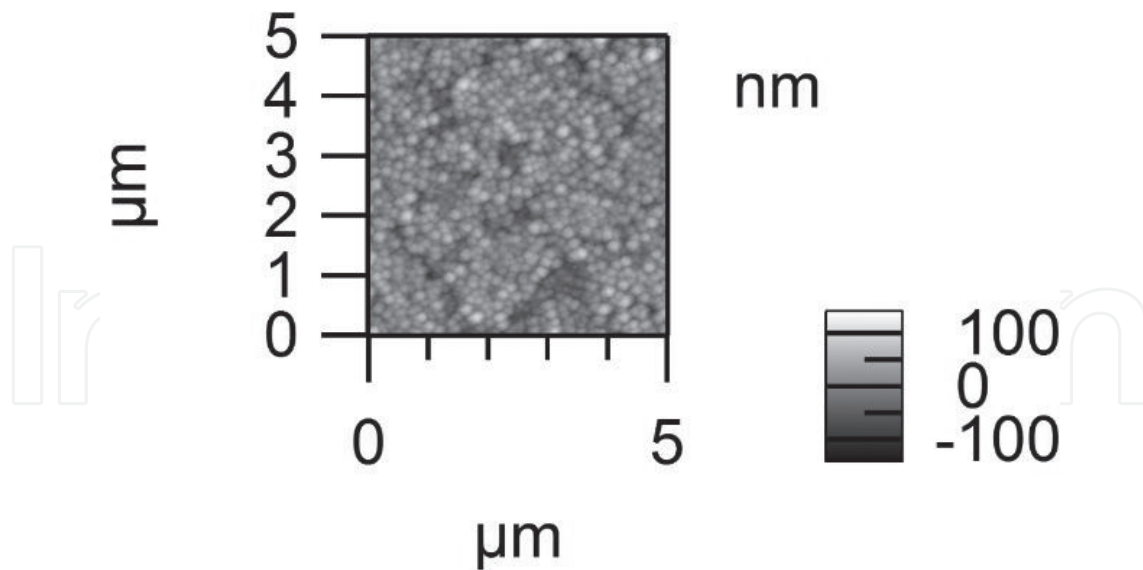


Figure 23. AFM characteristics of AuGeNi surface after Ar<sup>+</sup> ion beam sputtering.

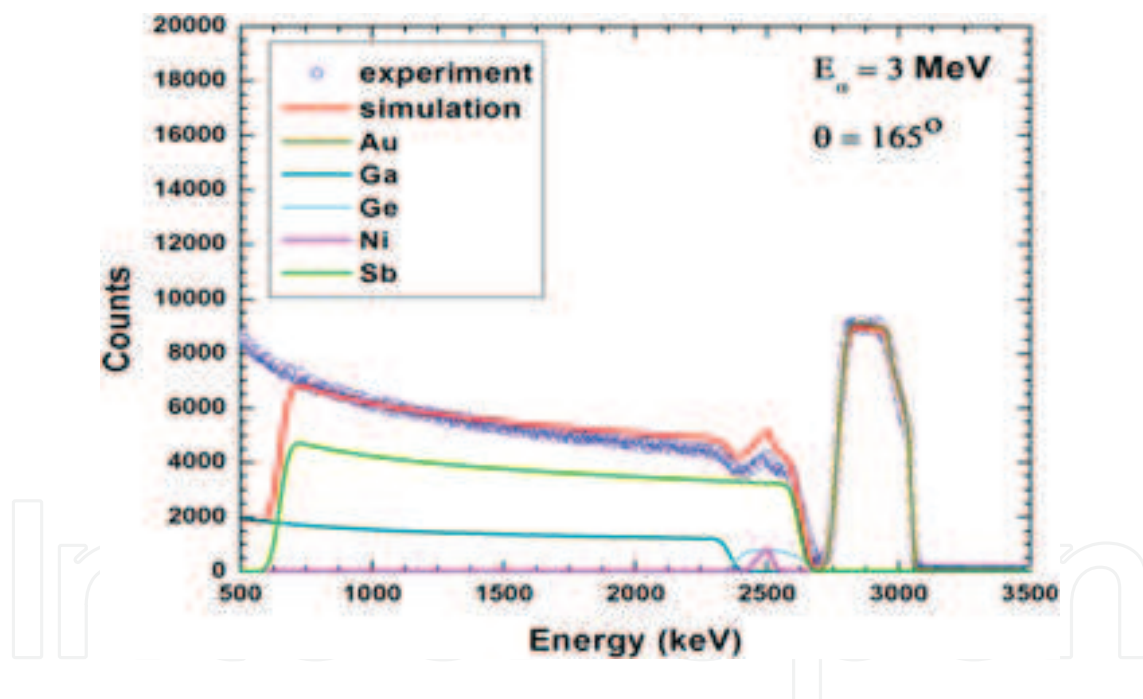
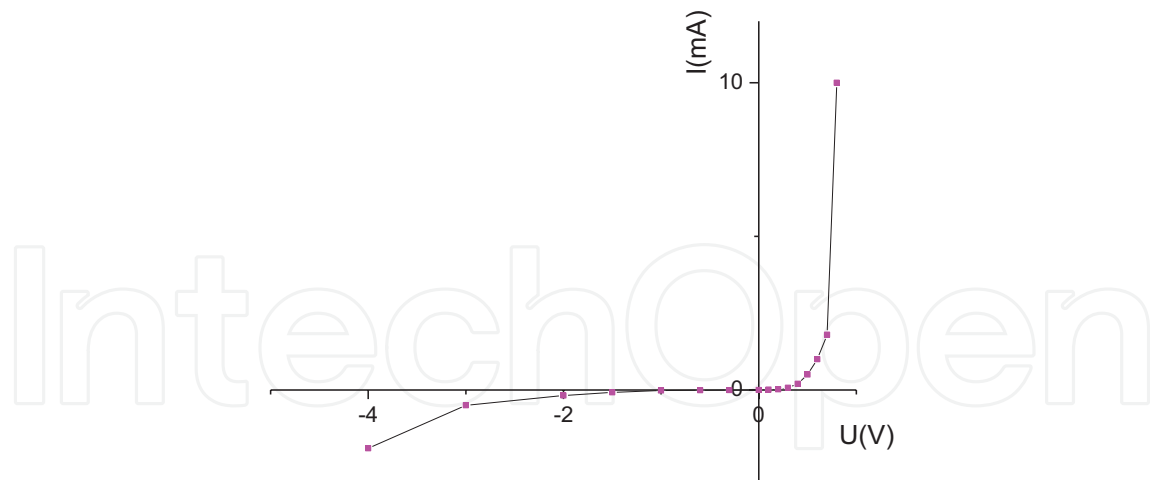


Figure 24. RBS spectrum of a AuGeNi deposited on n-GaSb substrate and a theoretical simulation for the elements present in the sample.

Gallium arsenide has been long time considered as one of the most important semiconductor material besides silicon, due to his attractive intrinsic electrical properties: direct energy and wider bandgap, higher carrier mobility, high power and operating temperature [33]. A key element in GaAs devices technology consists in the obtaining of high quality ohmic contacts because the surface of this compound is often covered with a chemically unstable oxide layer. Developed on a trial-and-error basis, the AuGeNi alloyed ohmic contacts remain the most widely used for n-GaAs devices manufacturing. This metallization system is characterized



**Figure 25.** I-V characteristics of a MBE Ni/GaSb Schottky contact (back side ohmic contact is AuGeNi).

by low contact resistance, good thermal stability both during device fabrication and device operation, strong adhesion, low metal sheet resistance [34]. In this system, namely AuGeNi/n-GaAs(110) [35], Au acts as a base metal and his role is to promote Ga vacancies in n-GaAs due to high solubility of Ga in Au. Ge acts as a dopant element, diffusing into the lattice sites vacated by Ga, creating in this way a heavily doped n-type intermediate semiconductor layer that allows the tunneling mechanism which leads to the ohmic behavior. Ni acts as a catalyst during the alloying procedure to improve the uniformity, thermal and mechanical stability, and a decrease of surface roughness [32]. **Figure 26** presents the depth profile of AuGeNi layer and the interface with the n-GaAs semiconductor. From this figure, it can be seen that while the As concentration tends to grow steadily, the Ga concentration varies in a different manner: it is greater in the first layers, then starts to decrease to a minimum of 35% and then is growing once more. This last growing is explained through the decrease of Au concentration which is more aggressively removed from the surface by ion sputtering. This indicates that both Ni and Ge diffuse deeper in the n-GaAs semiconductor. As presented in **Figure 27(a, b)**, XPS spectra for Ge  $3d$ , Au  $4f$  before sputtering, firstly for the Ge  $3d$ , the spectrum is composed from two peaks: one situated at 29 eV binding energy and the other situated at 32.2 eV. The first component, representing 32% from total peak area, is attributed to elemental Ge, while the second component, containing the rest of 68% from peak area, is attributed to  $\text{Ge}_2\text{O}_3$  specie. Even after the first sputtering session, the oxide completely disappears, remaining only the Ge metal component. The attempting to fit the Ge  $3d$  XPS recorded spectra with more than one peak provided unsatisfactory results and as a consequence the formation of other compounds, e.g.,  $\text{GeAs}_2$  or  $\text{Ni}_3\text{Ge}$  assigned to XPS BE of 29.7 and 29.1 eV is not realistic. From the XPS spectra Ni  $2p$  it is observed that Ni is missing in the first layers of the surface and the signal is arising from a metallic state.

Absence of shake up satellites indicates once more that Ni oxide is present in the layer. The evolution of Ni peak shape (e.g., close to the interface FWHM varies from 1.6 to 1.9 eV) is explained by the fact that a portion of Ni interacts directly with GaAs substrate in the semiconductor “wetting” process for which Ni role is intended. The presence of Ni even at

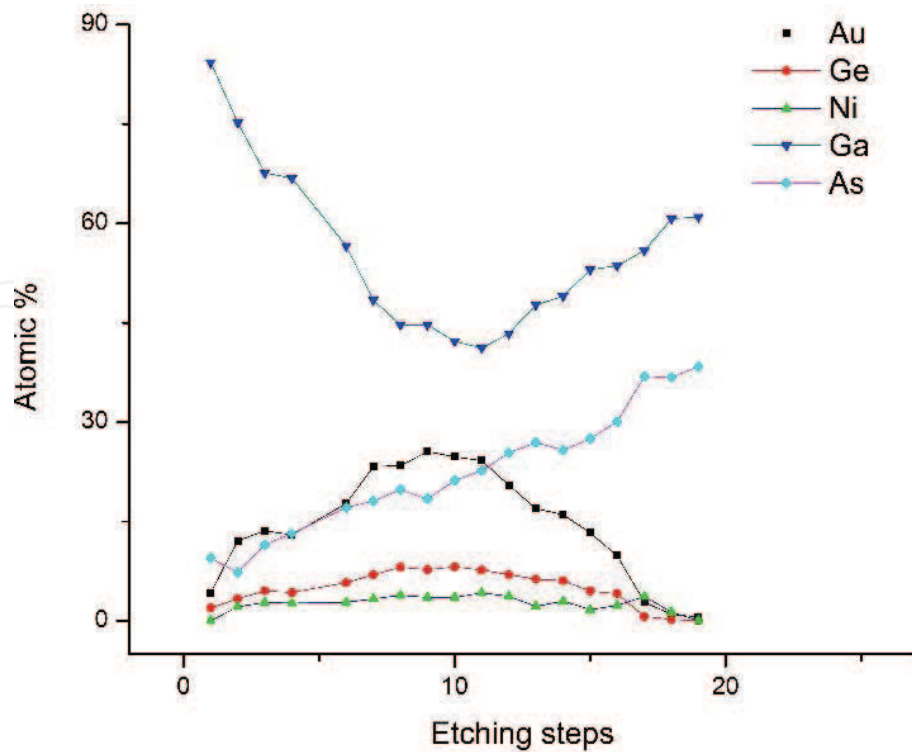


Figure 26. AuGeNi/n-GaAs profiling of chemical composition.

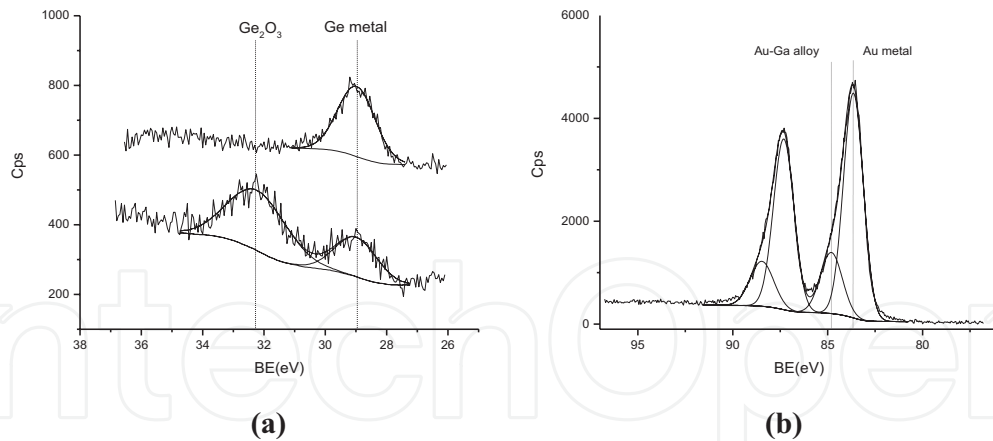


Figure 27. XPS spectra of (a) Ge 3d and (b) Au 4f at metal/semiconductor interface.

the interface is beneficial for the ohmic character of contacts in the sense that is reducing the lateral diffusion of Au and holds the Au-Ge melt in intimate contact with GaAs substrate during thermal annealing. From Au 4f XPS doublet recorded, it is remarked the gold from surface to the interface. Spectra fitting of  $4f^{7/2}$  line was made with two peaks, where the first one is attributed to the metallic gold Au  $4f^{7/2}$ , while the second is attributed to an alloy of Ga and Au [35], and the area of the second peak is less than a quarter of the total

area. The results indicated that the chemical shift of Au  $4f^{7/2}$  tends to be growing with the proportion of Ga, from 0.4 to 1.25 eV for AuGa, and 1.55 eV for AuGa<sub>2</sub> [36]. The chemical shift of 1.15 eV found in our experiment indicate more Au than Ga in the alloy but with close to 1 Ga/Au ratio. As a general remark Au, Ge and Ni are uniformly distributed in the metallic layer AuGeNi/n-GaAs(110) and both Ga and As diffuse to the surface, with a more pronounced Ga diffusion.

The as-prepared surface n-GaAs by controlled Ar<sup>+</sup> ion beam sputtering reveal the absence of native oxides and the metal deposition technique for obtaining good ohmic contacts is convenient and competitive to GaAs device technology.

## 6. Conclusions

Surface preparation of semiconductors, in particular, for III-V compounds is a necessary requirement in device technology due to the existence of surface impurities and the presence of native oxides. The impurities can affect the adherence of ohmic and Schottky contacts and due to the thermal decomposition of native oxides (e.g., GaSb) it also affect the interface metal/semiconductor. The practical experience reveals that the simple preparation of a surface is a nonrealistic expectation, i.e., surface preparation is a result of combined treatments. In this view, the ion beam sputtering surface preparation is an efficient technique that removes rapidly and in *in situ* the native oxides. The effect of major cleaning of semiconductor surface is accomplished, however, by surface damaging. The removal of surface damage is obtained by cycles of thermal annealing at a relative high temperature. It is worth to mention GaSb or GaAs III-V compounds, the ion beam etching leaves a surface enriched in Ga atoms, that means the presence of a nonstoichiometric characteristic. In the case of chemical etching preparation, the etchants generally specific to the semiconductor are selective in respect to the crystallographic plane (i.e., the etch rate different). The chemical etching is an effective and rapid *ex situ* preparation technique that can leave a slightly nonstoichiometric surface (e.g., there exists a depletion in Ga atoms). Also, the chemical etching leaves traces of native oxide. In this stage, the preparation includes thermal treatments, but the annealing implies a temperature lower than in case of ion beam cleaning.

The efficient technological method for III-V compounds surface preparation is considered to be the combination between chemical etching and controlled thermal treatment. The effect of surface preparation can be observed by XPS for the surface chemical quality, by AFM for surface morphology, and by LEED for the structural characteristics.

## Acknowledgements

The authors thank for the financial support provided by the Ministry of Education from Romania-UEFISCDI Project No. 68/2014-Partnerships.

## Author details

Rodica V. Ghita\*, Constantin Logofatu, Constantin-Catalin Negrila, Lucian Trupina and Costel Cotirlan-Simioniuc

\*Address all correspondence to: [ghitar@infim.ro](mailto:ghitar@infim.ro)

National Institute of Materials Physics, Bucharest, Romania

## References

- [1] I. Vurgaftman, J.R. Meyer, and L.R. Ram-Mohan, *J. Appl. Phys.*, 89, 5815 (2001).
- [2] K. Nakahara et al., *Electron. Lett.*, 32, 1585 (1996).
- [3] P.S. Dutta, H.L. Bhat, and V. Kumar, *J. Appl. Phys.*, 81, 5821 (1997).
- [4] G. Motosugi and T. Kagawa, *Jpn. J. Appl. Phys.*, 19, 2303 (1980).
- [5] O. Hildebrand, W. Kuebant, and M.H. Pilkuhn, *Appl. Phys. Lett.* 37, 80 (1980).
- [6] C. Hilsum and H.D. Rees, *Electron. Lett.*, 6, 277 (1970).
- [7] L.M. Fraas, G.R. Girard, J.E. Avery, B.A. Arau, V.S. Sundaram, A.G. Thomson, and J.M. Gee, *J. Appl. Phys.*, 66, 3866 (1989).
- [8] C. Cotirlan, C. Logofatu, C.C. Negrila, R.V. Ghita, A.S. Manea, and M.F. Lazarescu, *J. Optoelectron Adv. Mater.*, 11(4), 386 (2009).
- [9] J.W. Faust Jr. in "The Surface Chemistry of Metals and Semiconductors" (H.C. Gatos ed), Wiley, New York, 1960.
- [10] H.C. Gatos and M.C. Lavine, *Prog. Semicond.*, 9, 1 (1965).
- [11] P.R. Camp, *J. Electrochem. Soc.*, 102, 586 (1955).
- [12] A.M. Morgan and I. Dalins, *J. Vac. Sci. Technol.*, 10, 523 (1973).
- [13] D. Klinov, B. Dwir, E. Kapon, N. Borovok, T. Molotsky, and A. Kotlyar, High-resolution atomic force microscopy of duplex and triplex DNA molecules, *Nanotechnology*, 18 (2007) 225102 (8pp) doi:10.1088/0957-4484/18/22/225102.
- [14] L.R. Doolittle, *NIMB*, 15, 227 (1986).
- [15] J. Makela, M. Tuominen, M. Yasir, M. Kuzmin, J. Dahl, M.P.J. Punkkinen, P. Laukkanen, K. Kokko, and R.M. Wallace, *Appl. Phys. Lett.*, 107, 061601 (2015).
- [16] Hartman et al. United States Patent, No. 4227975 (Oct. 14, 1980).
- [17] O. El-Atwani, J.P. Allain and A. Suslova, *Appl. Phys. Lett.* 101, 251606 (2012).



- [18] G.P. Schwartz, G.P. Gualtieri, J.E. Griffiths, C.D. Thurmond, and B. Schwartz, *J. Electrochem. Soc.* 127, 2488 (1980).
- [19] O. El-Atwani, J.P. Allain, A. Cimaroli, A. Suslova, and S. Ortoleva, *J. Appl. Phys.* 110, 07301 (2011).
- [20] Freiberger. General Specifications, Issue 2000 ([www.fem-semicond.com/pdf/gen.spec.pdf](http://www.fem-semicond.com/pdf/gen.spec.pdf)).
- [21] C.C. Negrila, C. Logofatu, R.V. Ghita, C. Cotirlan, F. Ungureanu, A.S. Manea, and M.F. Lazarescu, *J. Cryst. Growth*, 310, 1576 (2008).
- [22] R.V. Ghita, C. Negrila, A.S. Manea, C. Logofatu, M. Cernea, and M.F. Lazarescu, *J. Optoelectron. Adv. Mater.*, 5(4), 859 (2003).
- [23] E. Papis-Polakowska, *Electron Technology-Internet Journal*, 37/38 1 (2005/2006).
- [24] W.E. Spicer, I. Lindau, P. Pianetta, P.W. Chye, and C.M. Garner, *Thin Solid Films*, 56, 1 (1978).
- [25] H. Iwasaki, Y. Mizokawa, and S. Nakamura, *Jpn. J. Appl. Phys.*, 18, 1525 (1979).
- [26] C. Cotirlan, R.V. Ghita, C.C. Negrila, C. Logofatu, F. Frumosu, and G.A. Lungu, *Appl. Surf. Sci.*, 363, 83 (2016).
- [27] C.C. Surdu-Bob, S.O. Saied, and J.L. Sullivan, *Appl. Surf. Sci.*, 183, 126 (2001).
- [28] V.N. Bessolov, M.V. Lebedev, N.M. Binh, M. Friedrich, and D.R.T. Zahn, *Semicond. Sci. Technol.*, 13, 611 (1998).
- [29] J.L. Sullivan, W. Yu, and S.O. Saied, *Sur. Interface. Anal.*, 22, 515 (1994).
- [30] J.S. Pan, A.T.S. Wee, C.H.A. Huan, H.S. Tan, and K.L. Tan, *J. Phys. D: Appl. Phys.*, 30, 2514 (1997).
- [31] J.S. Williams, *Rep. Prog. Phys.*, 49, 491 (1986).
- [32] M. Murakami, *Science and Technology of Advanced Materials*, 3, 1, (2002).
- [33] M. R. Brozell and C.E. Stillman, *Properties of Gallium Arsenide*, INSPEC, Institution of Electrical Engineers, University of Michigan, Third Edition, (1996).
- [34] A. Baca, F. Ren, J. Zolper, R. Briggs, and S. Pearton, *Thin Solid Films*, 308–309, 599 (1997).
- [35] C.C. Negrila, M.F. Lazarescu, C. Logofatu, C. Cotirlan, R.V. Ghita, F. Frumosu, and L. Trupina, *J. Nanomater.*, 2016, ID 7574526 (2016).
- [36] D.T. Jayne, N.S. Fatemi, and V.G. Weizer., *J. Vac. Sci. Technol. A.*, 10, 2802 (1992).